PASI

Volcanic gas studies to infer magma dynamics, transport and storage

Mike Burton

Istituto Nazionale di
Geofisica e Vulcanologia
Pisa, Italy

- Critical role of gases in volcanic and other processes
- Gas measurement techniques
- Volatile exsolution, degassing processes, quiescent degassing
- Supercritical fluids
- Constraints on source processes for geophysical and volcanological observations
- Endogenous growth of volcanoes

Volatiles are prime drivers of volcanic activity

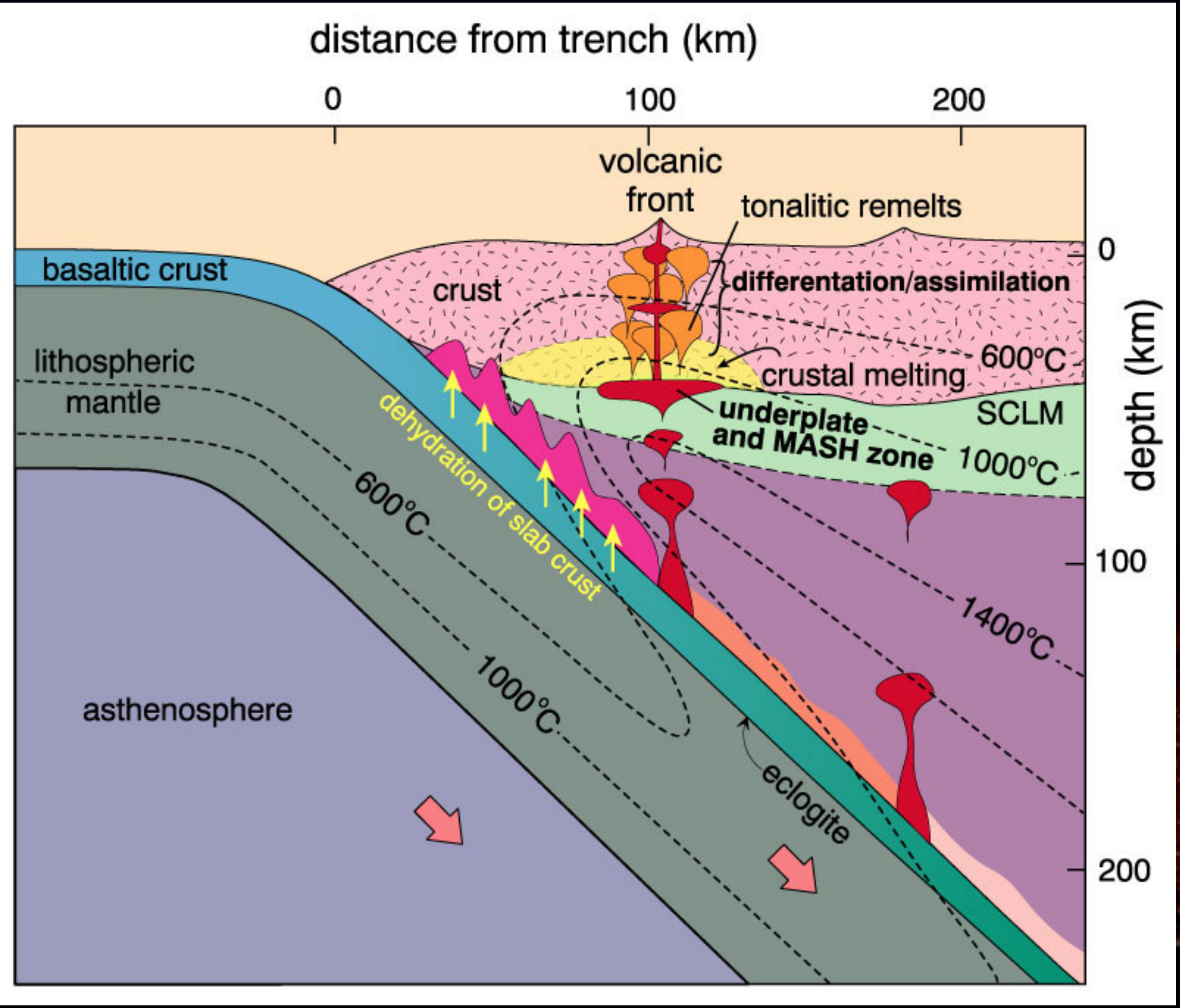

Volatiles are prime drivers of volcanic activity

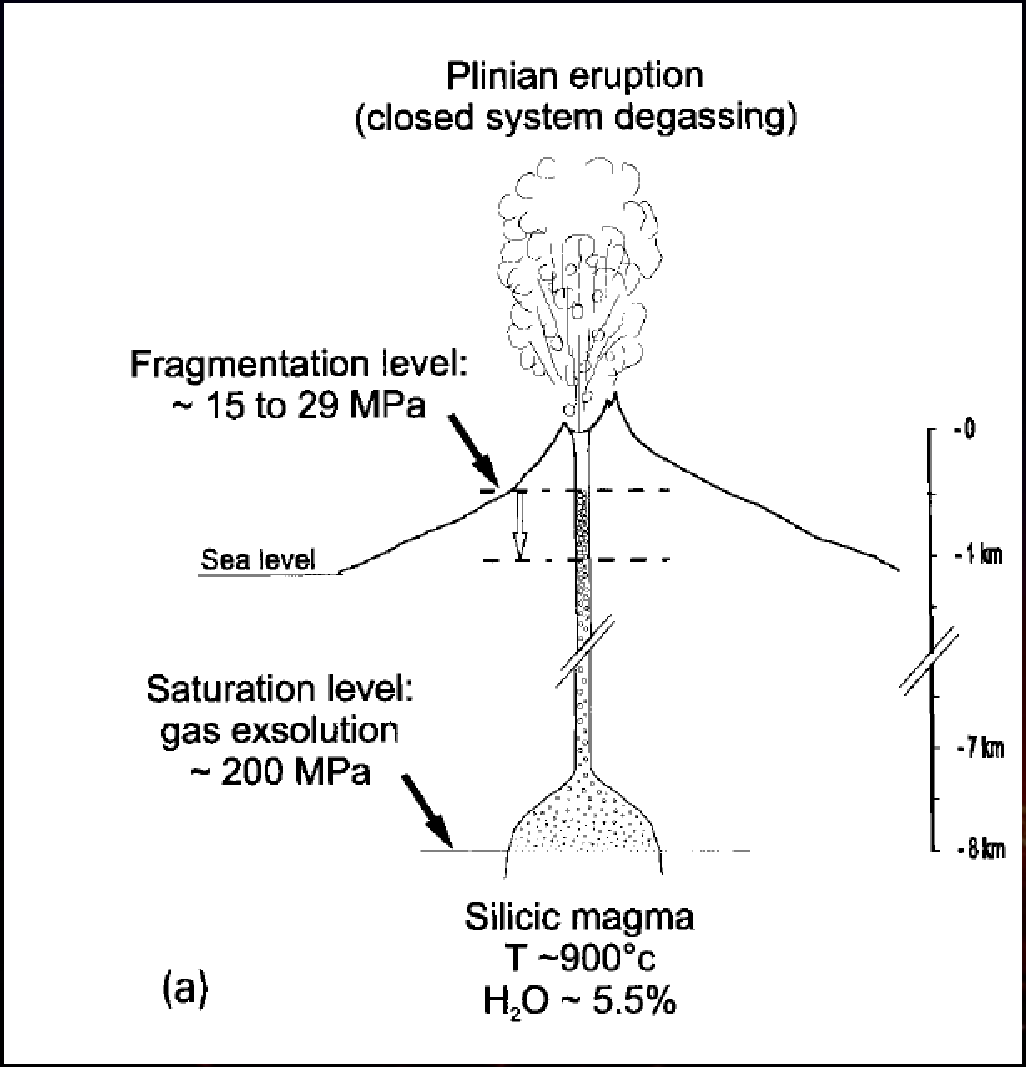

Villemant and Boudon, EPSL, 1999

Volatiles are prime drivers of volcanic activity

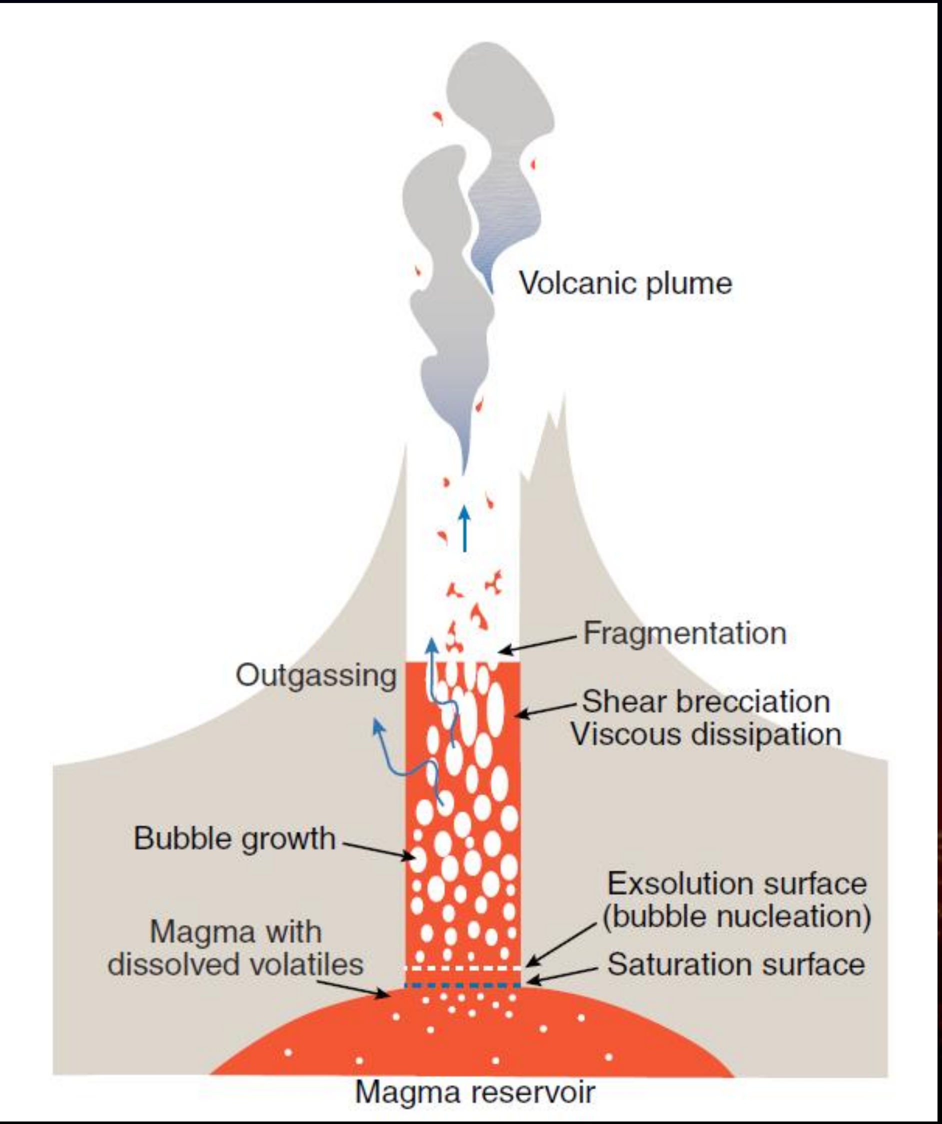

Volcanic degassing plays a major role in Earth's climate, particularly through CO2

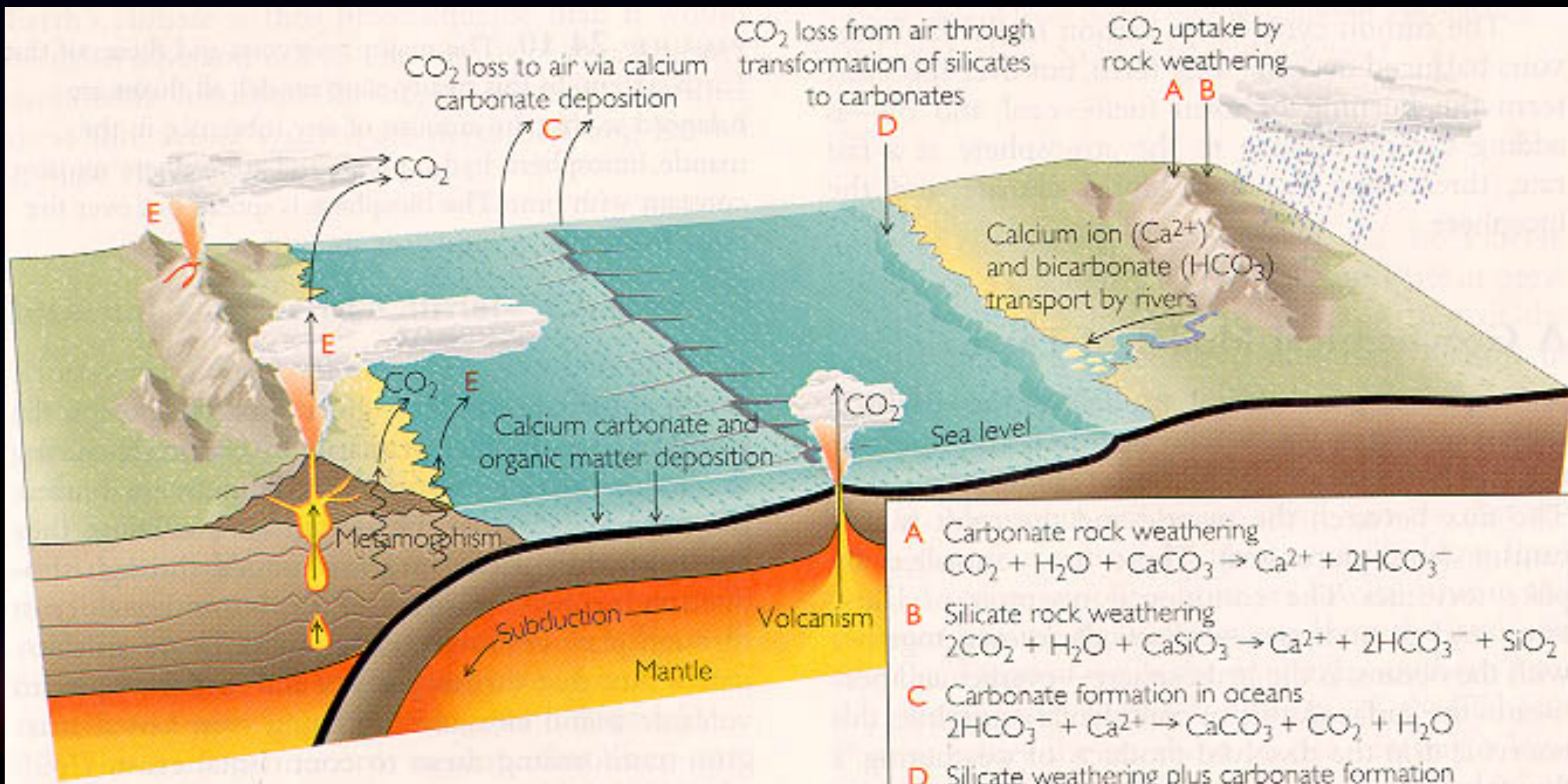

Sources, Reservoirs, and Fluxes of Carbon in the Earth System. Letters indicate the prevalent chemical reactions.

Volcanic gas compositions reflect mantle melting processes

Volcano Tectonic Style Temperature	**Kilauea Summit** Hot Spot 1170°C	**Erta` Ale** Divergent Plate 1130°C	**Momotombo** Convergent Plate 820°C
H_2O	37.1	77.2	97.1
CO_2	48.9	11.3	1.44
SO_2	11.8	8.34	0.50
H_2	0.49	1.39	0.70
CO	1.51	0.44	0.01
H_2S	0.04	0.68	0.23
HCl	0.08	0.42	2.89

From Symonds et al., 1994

Volcanic gas compositions reflect crustal-magma interactions

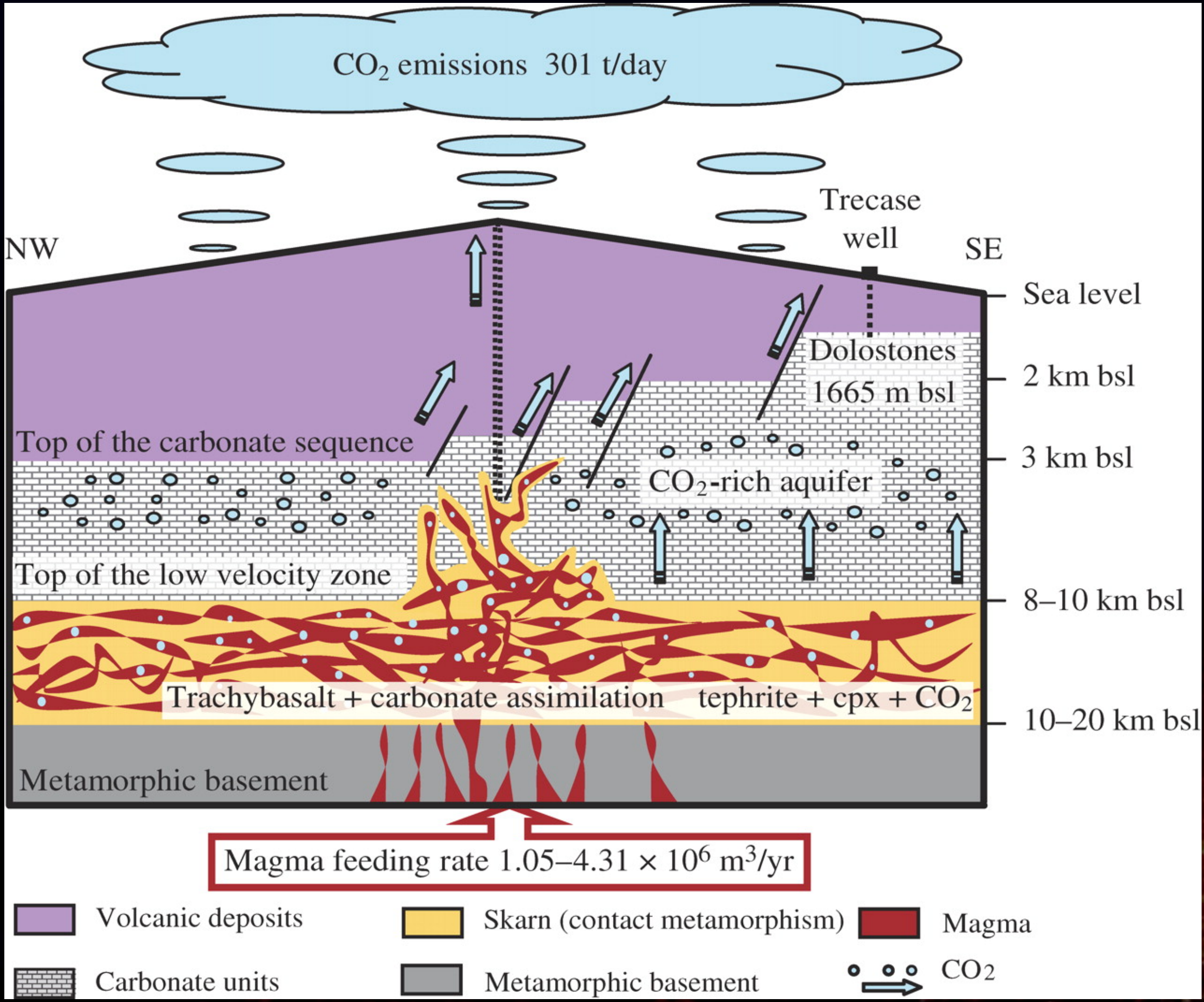

Iacono-Marziano et al., Role of non-mantle CO2 in the dynamics of volcano degassing: The Mount Vesuvius example Geology 2009,

Volcanic gases mediate geophysical phenomena

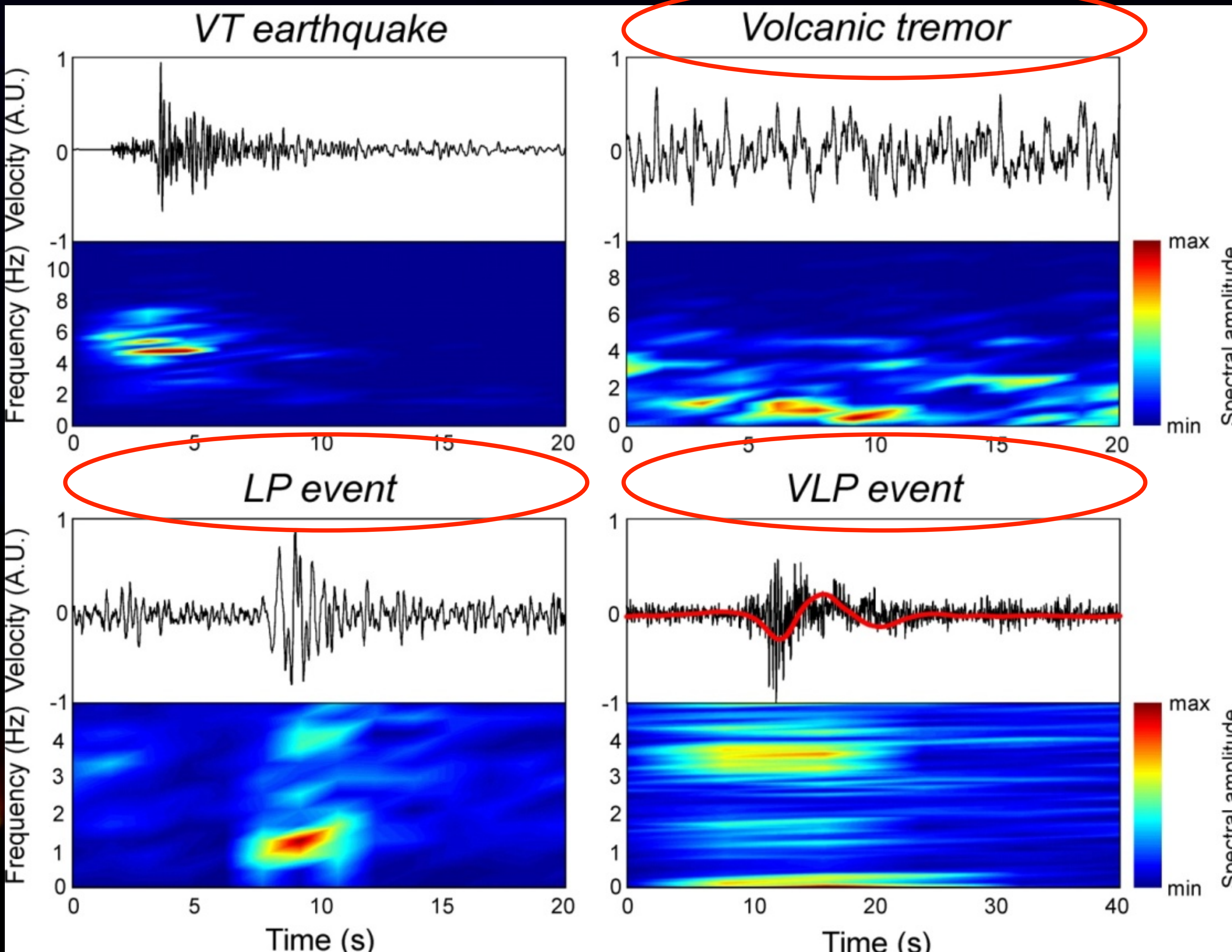

Volcanic gas fluxes are controlled by magma fluxes

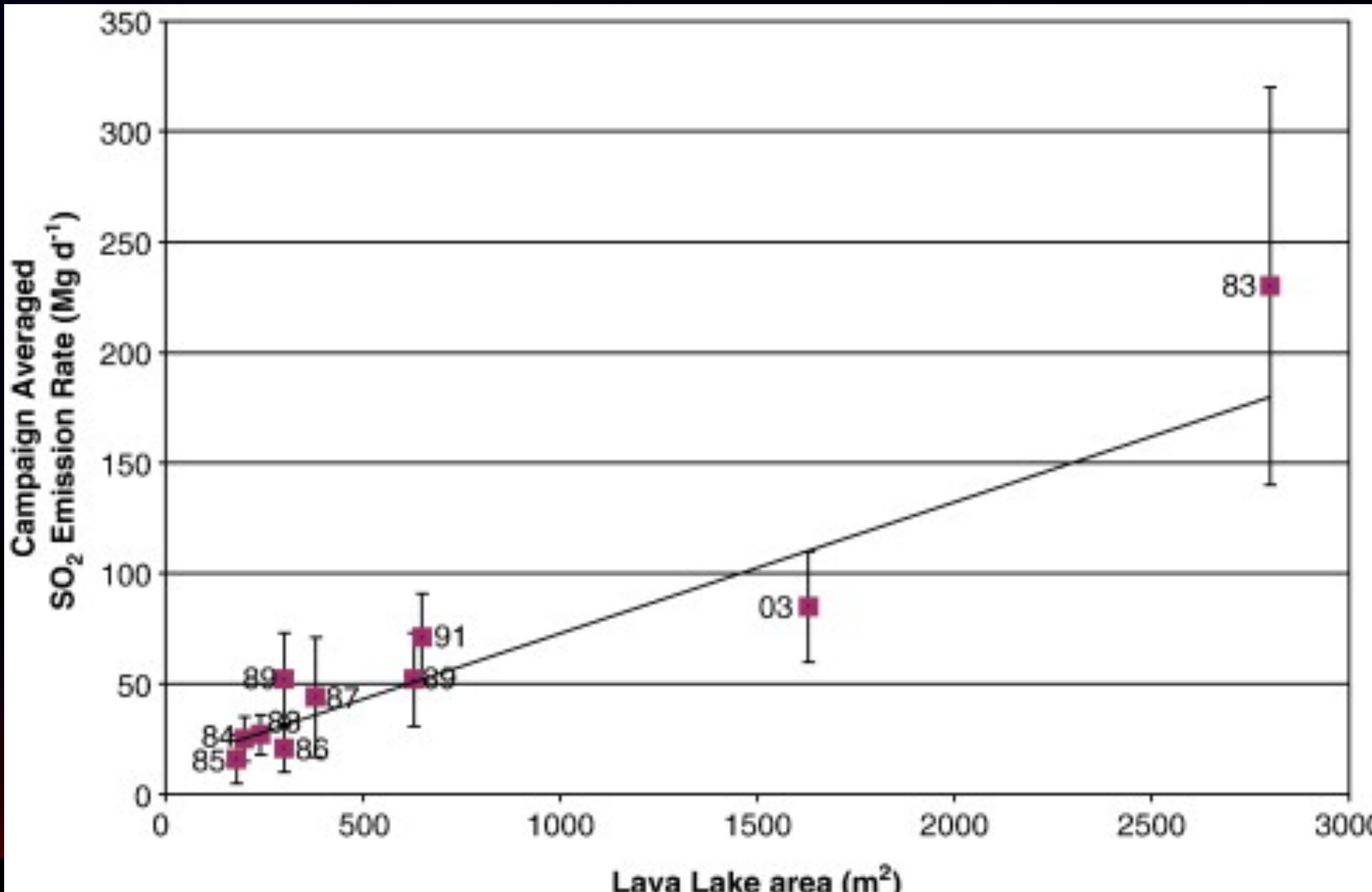

Mt. Erebus, Antarctica, Sweeney et al., JVGR, 2008

Supercritical H_2O and CO_2

The main components of magmatic gases are H_2O and CO_2

These gases are often modelled as ideal gases, whose density increases linearly with pressure.

Instead, they are non-ideal, supercritical fluids at magmatic temperatures and pressures.

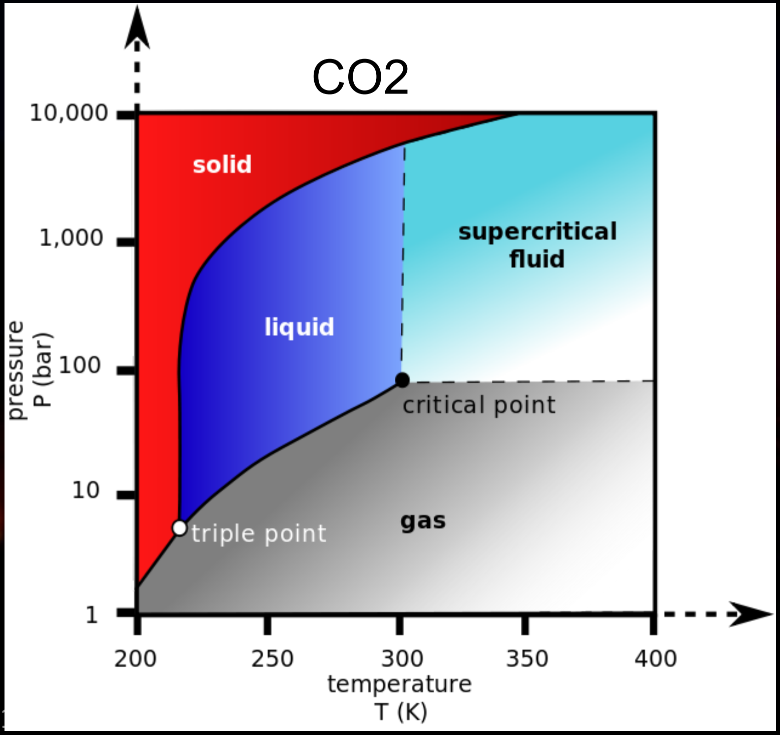

Supercritical H2O and CO2

Solvent	Molecular weight g/mol	Critical temperature K	Critical pressure MPa (atm)	Critical density g/cm^3
Carbon dioxide (CO_2)	44.01	304.1	7.38 (72.8)	0.469
Water (H_2O) (acc. IAPWS)	18.015	647.096	22.064 (217.755)	0.322

At critical point H2O is 4.4 times denser than an ideal gas, and CO2 3.6 times

Supercritical H2O and CO2

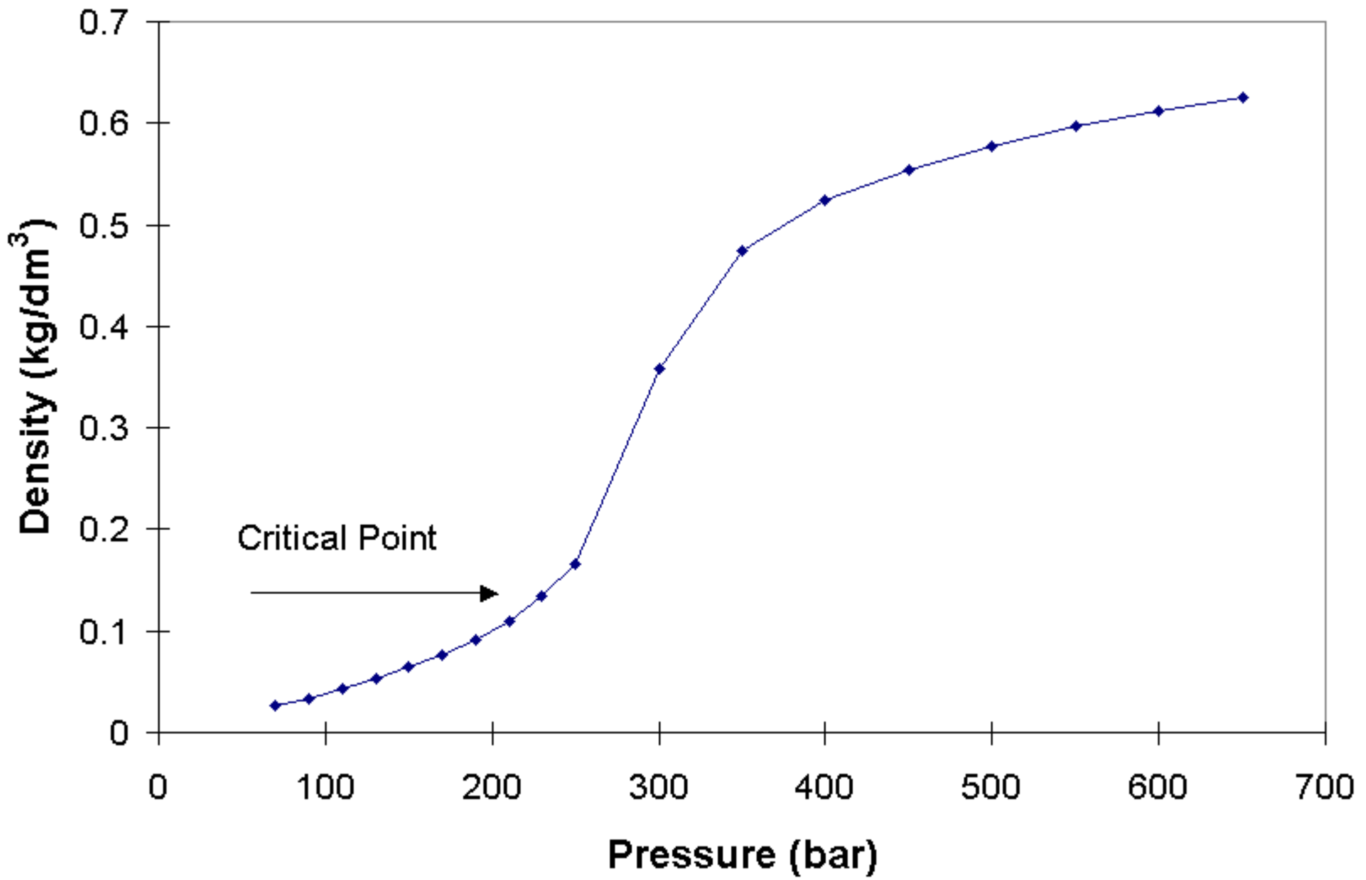

Figure 2: Pressure-Density Diagram for Water at 400°C

Water density is highly non-linear wrt P

Volcanic gas measurement techniques

- Gas flux
- Gas composition

- Gas sampling
- In-situ direct measurement
- Remote sensing, from ground, air and space

Gas Sampling: Giggenbach bottles

Gas Sampling: Filter Packs

Gas Sampling: Pumping CO2 into dry bags

In-situ direct measurements: MultiGas

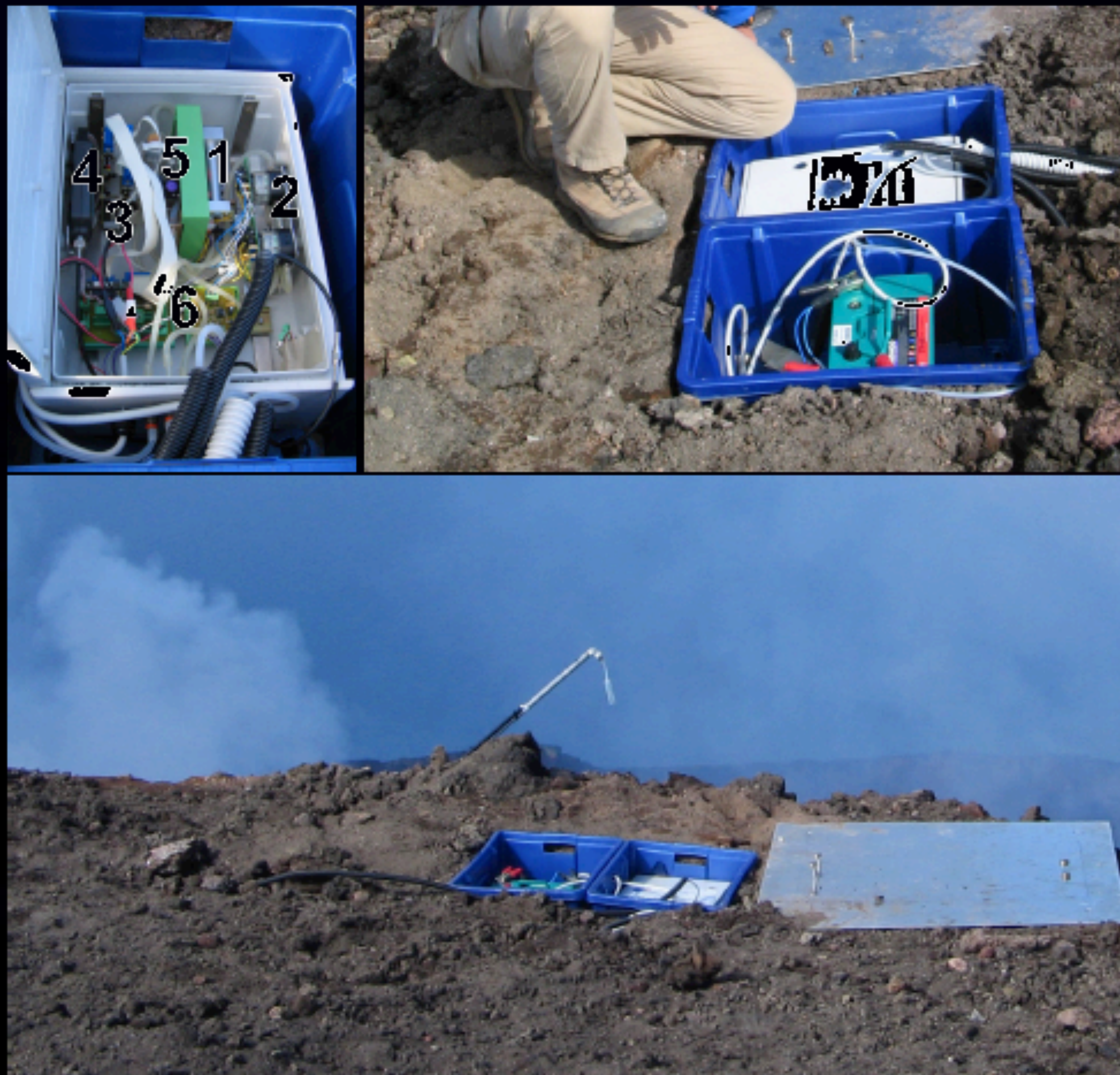

In-situ direct measurements: Soil Gas CO2 flux

Remote sensing: Space

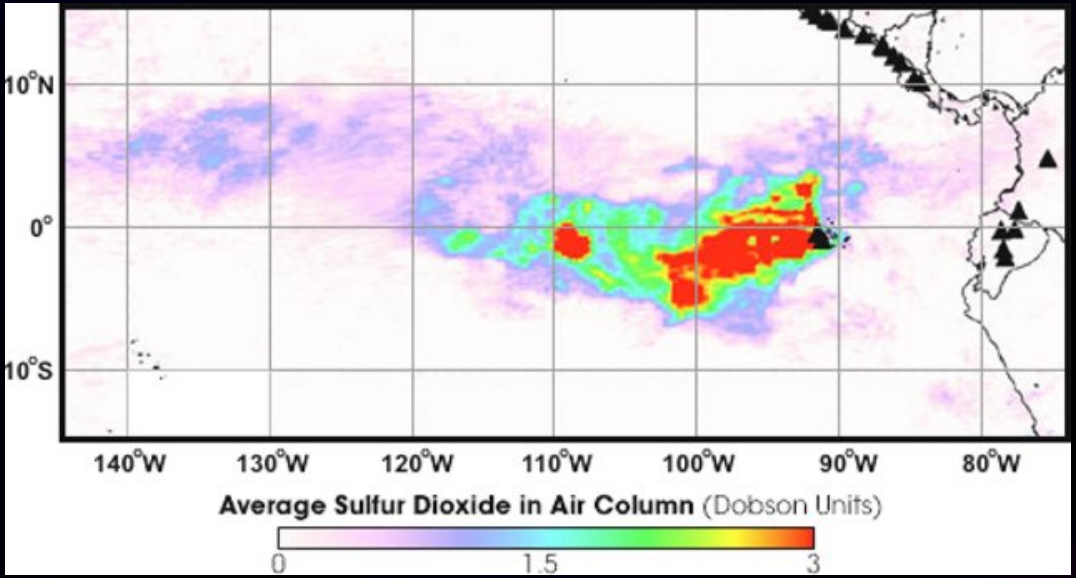

OMI

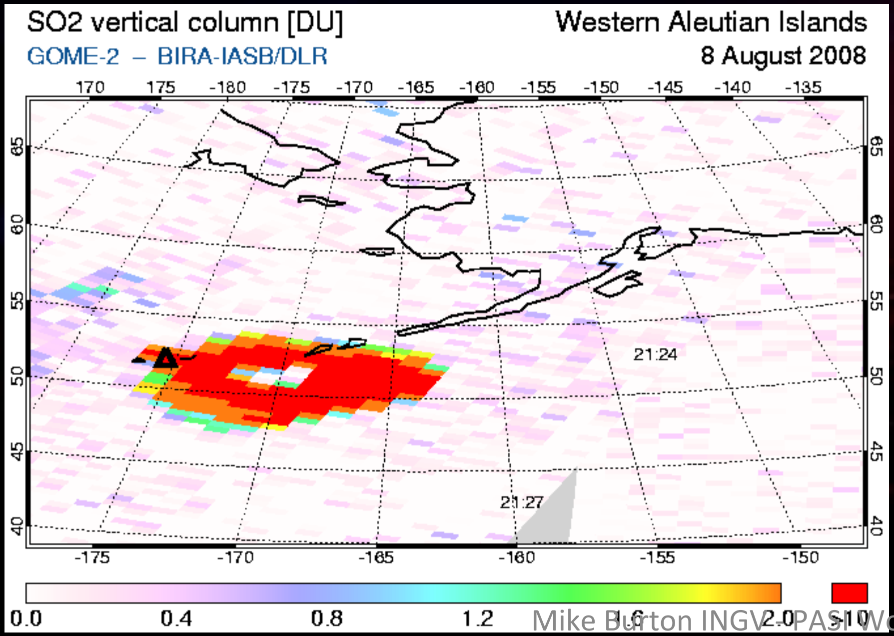

GOME-2

Retrieving time series of SO2 emissions from MODIS imagery: Mt. Etna

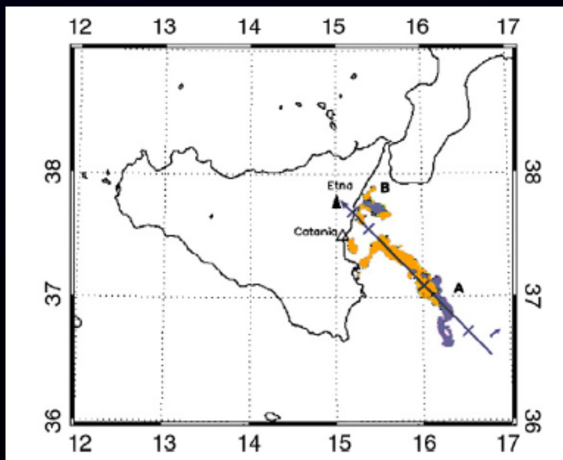

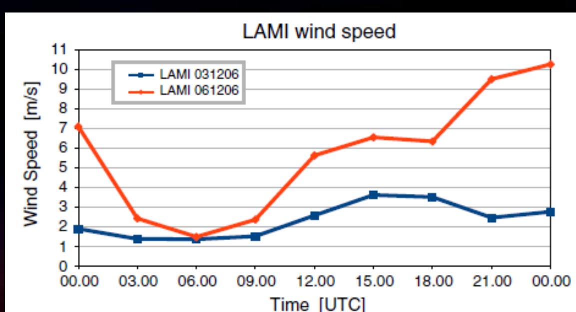

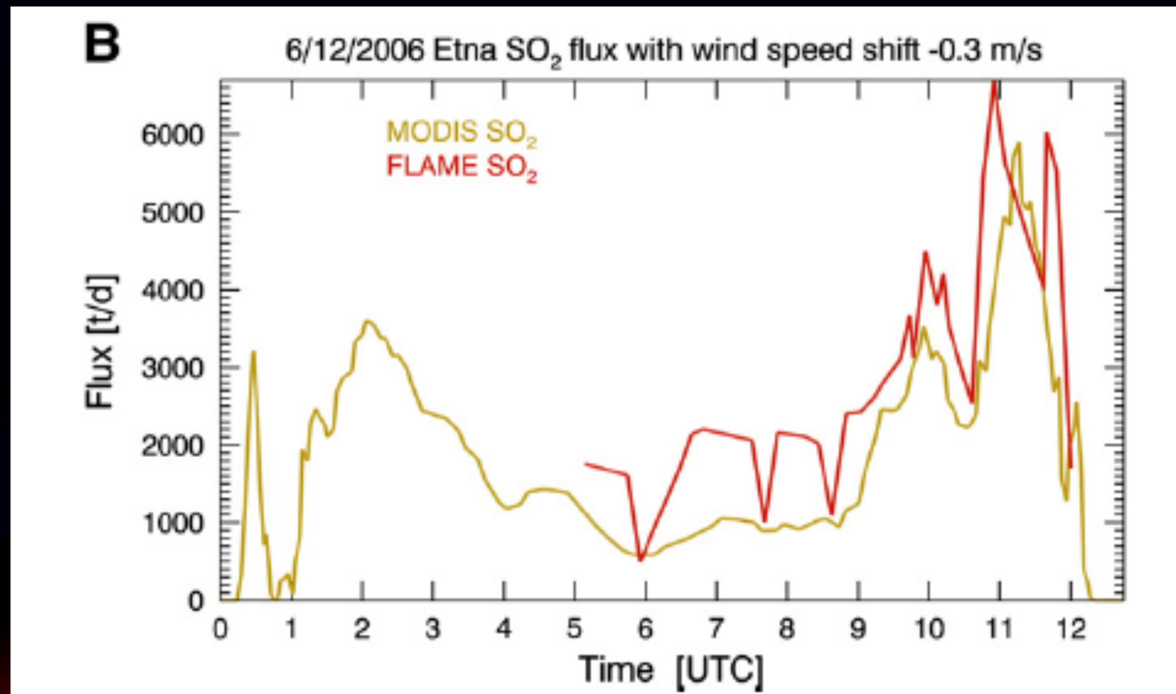

Fig. 5. MODIS and FLAME SO_2 flux comparison for the best matching wind speed offsets found by inspection for (A) 3rd of December 2006 and (B) 6th of December 2006 eruption events.

Reconstruction of SO_2 flux emission chronology from space-based measurements

Luca Merucci [a,*], Michael Burton [b], Stefano Corradini [a], Giuseppe Giovanni Salerno [c]

L. Merucci et al. / Journal of Volcanology and Geothermal Research 206 (2011) 80–87

Remote sensing: Beer-Lambert Law

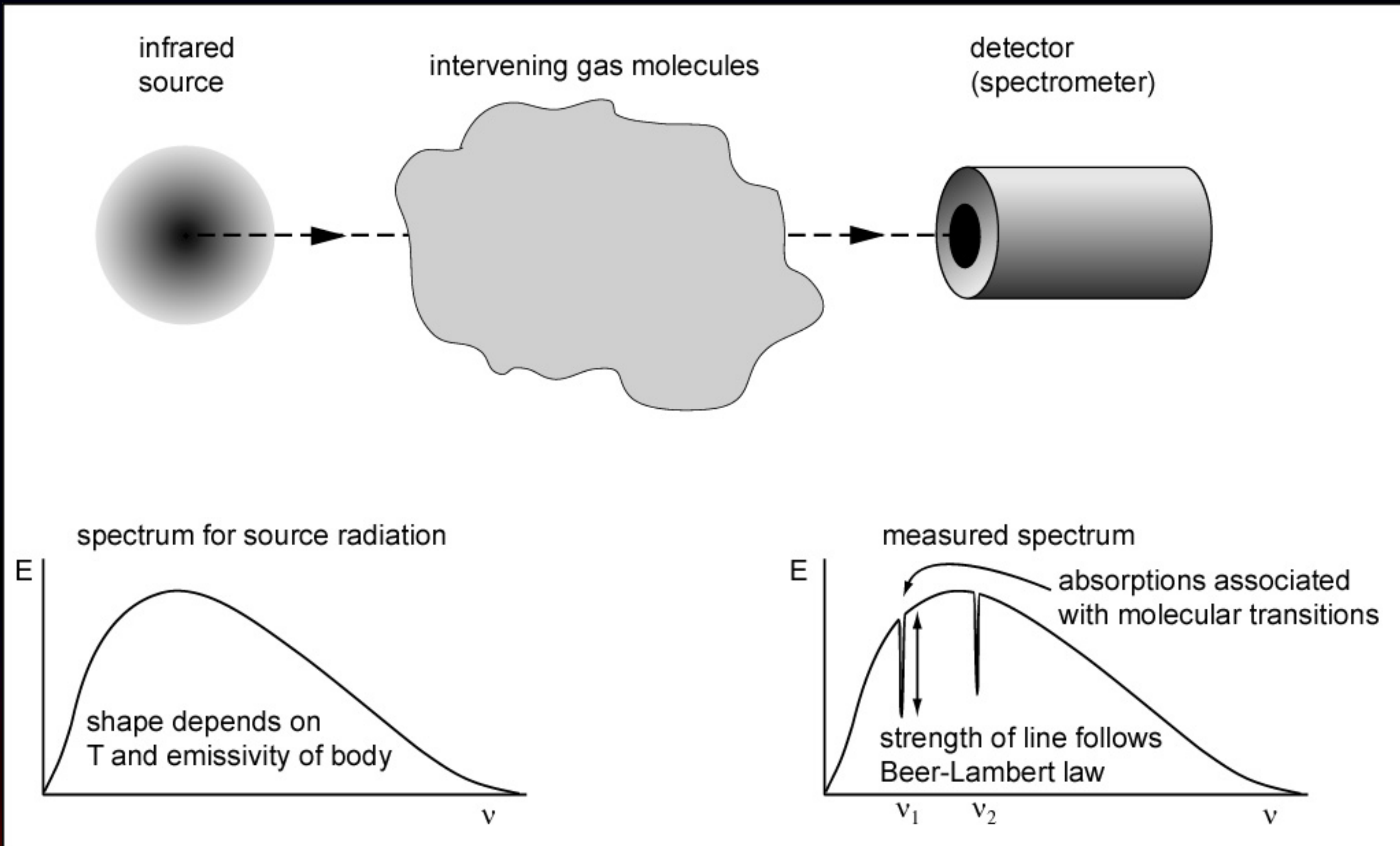

Remote sensing: Beer-Lambert Law

Transmittance is $I/I_0 = \exp(-\varepsilon cl) = \tau$

Therefore observed intensity is $I_0.\exp(-\varepsilon cl) = I_0.\tau$

Adding more gases produces a multiplicative effect, e.g.

$$I = I_0.\tau_{gas1}.\tau_{gas2}.\tau_{gas3}.\tau_{gas4}\cdots$$

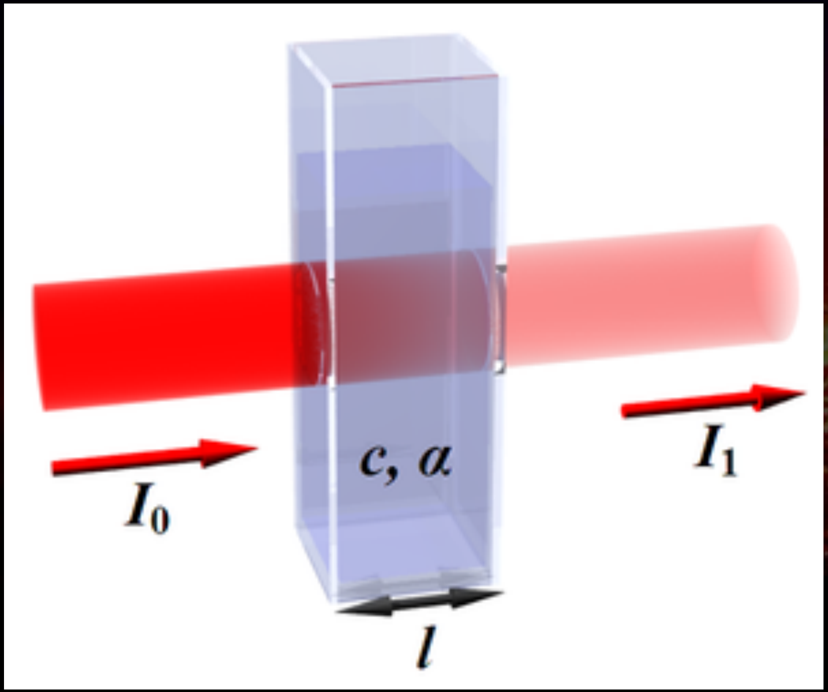

Remote sensing: SO2 flux

Remote sensing: SO2 flux

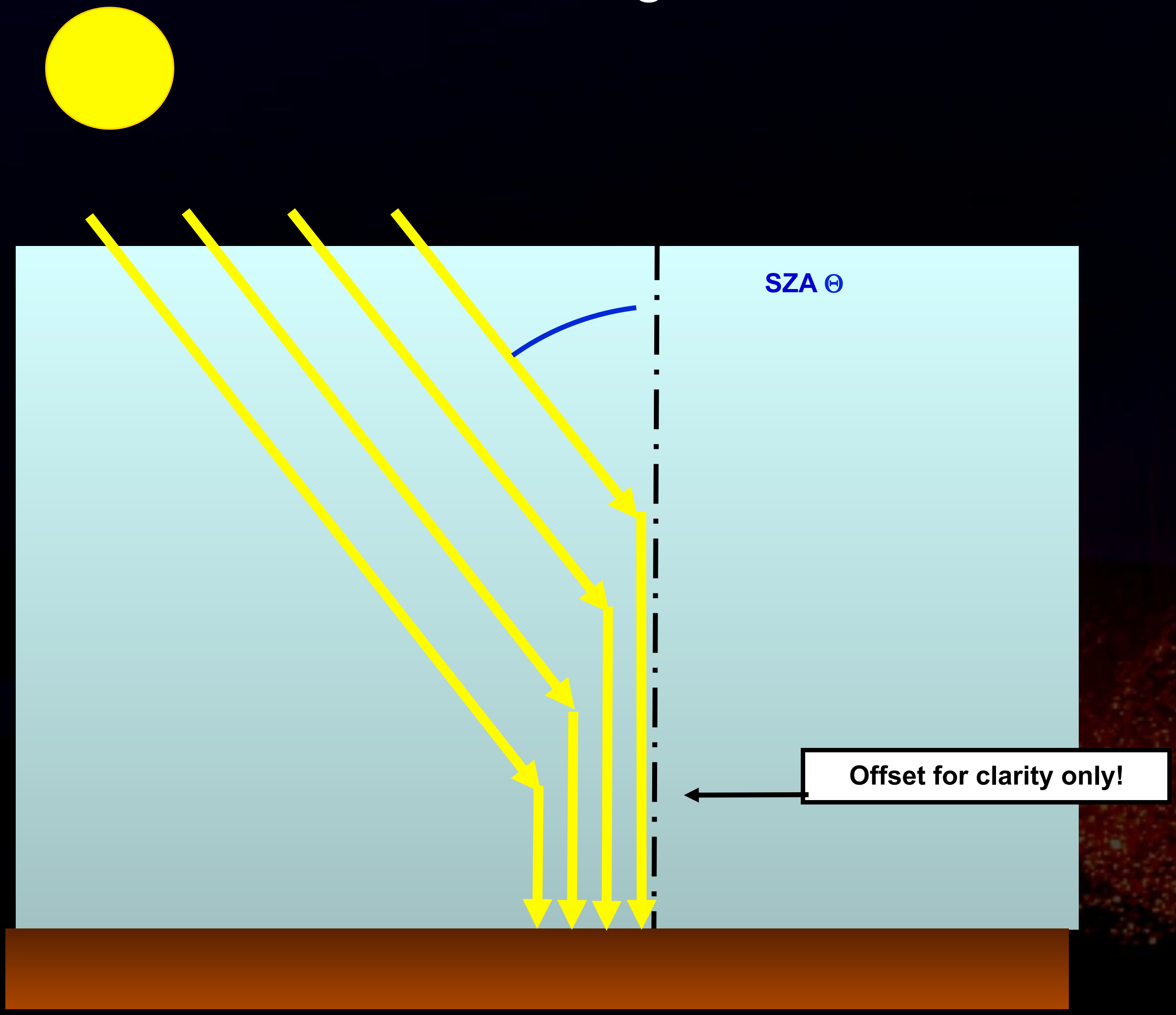

Remote sensing: SO2 flux

Remote sensing: SO2 flux

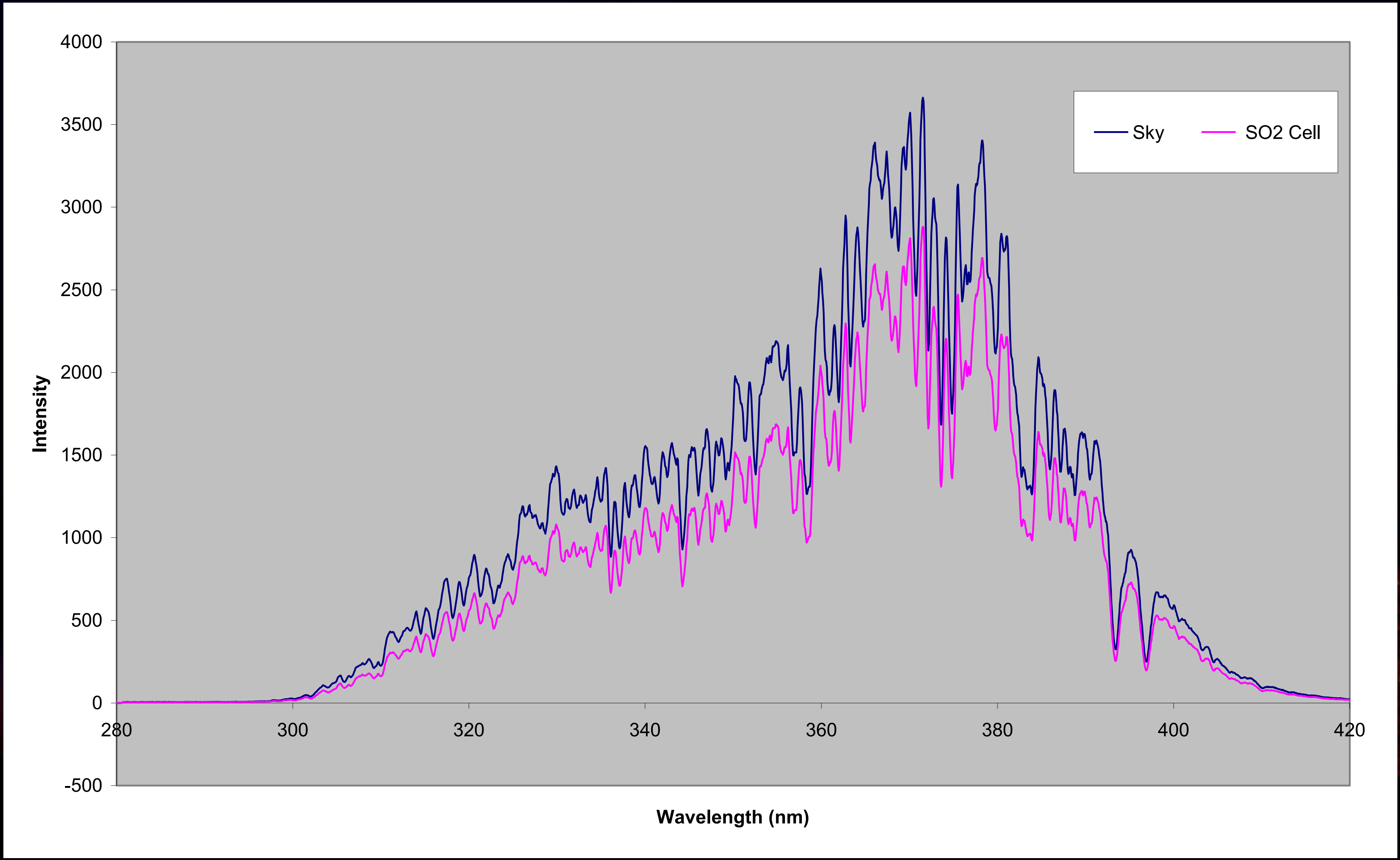

Remote sensing: SO2 flux

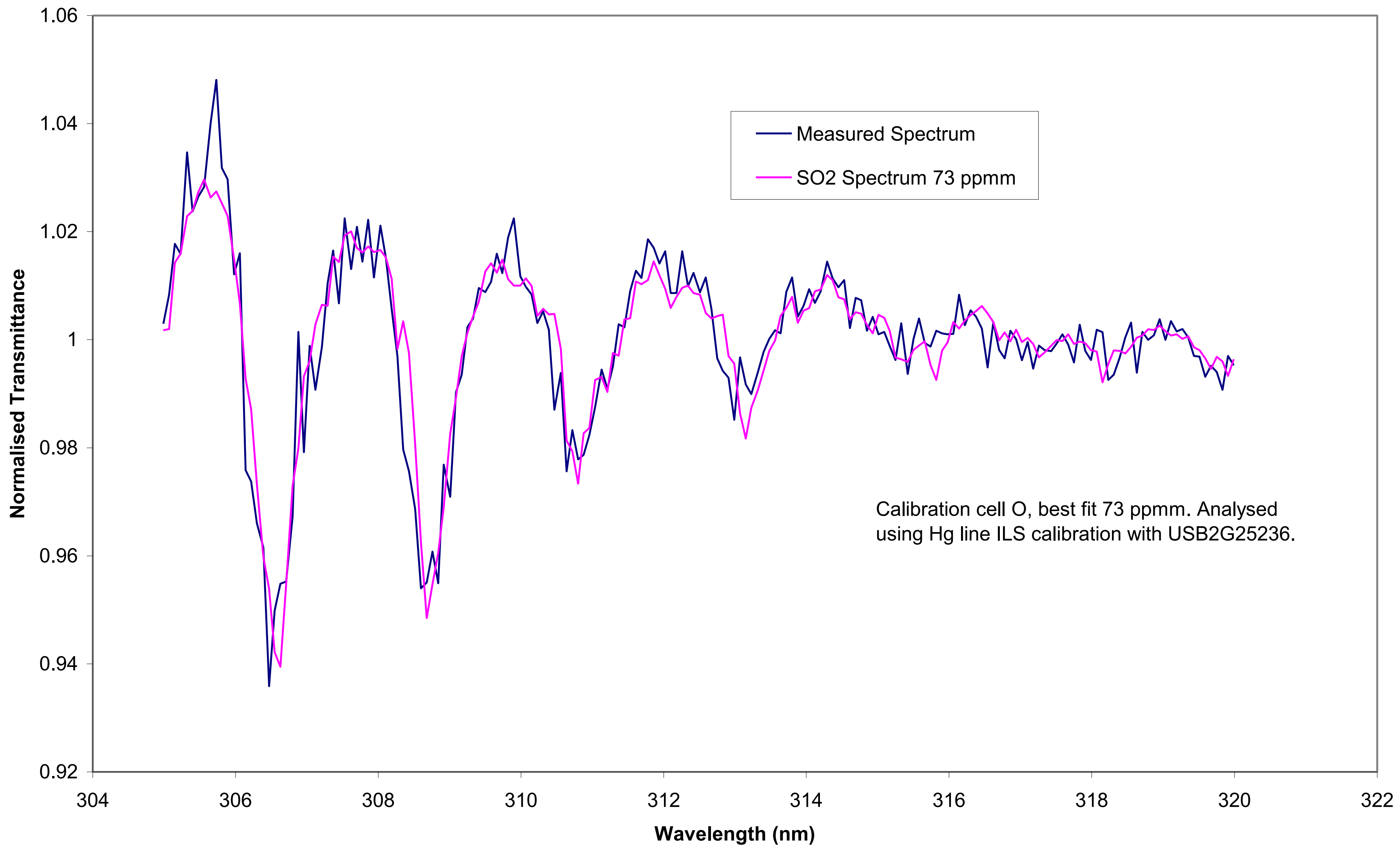

Technology for measuring SO2

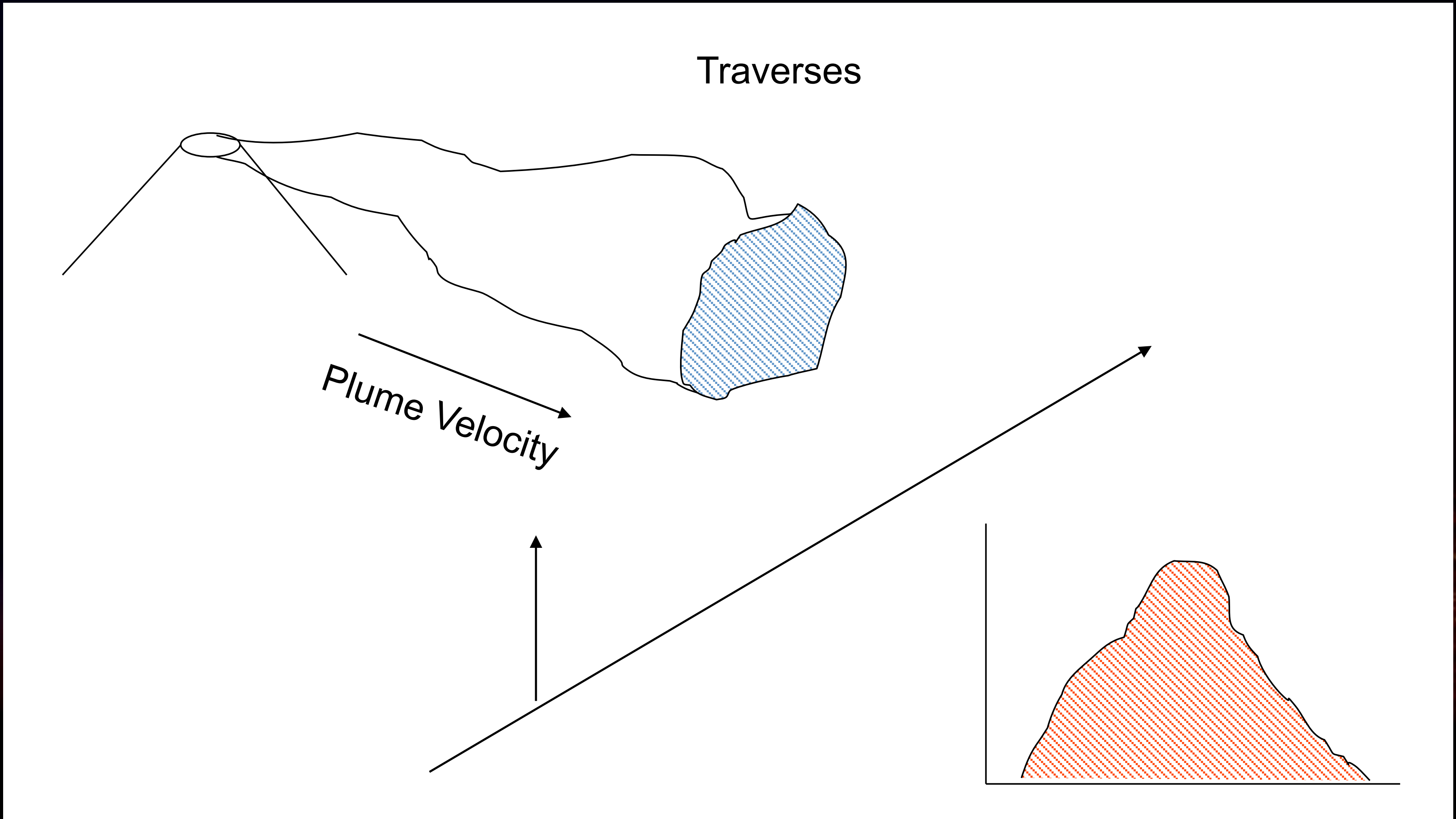

Technology for measuring SO2

Technology for measuring SO2

Technology for measuring SO2

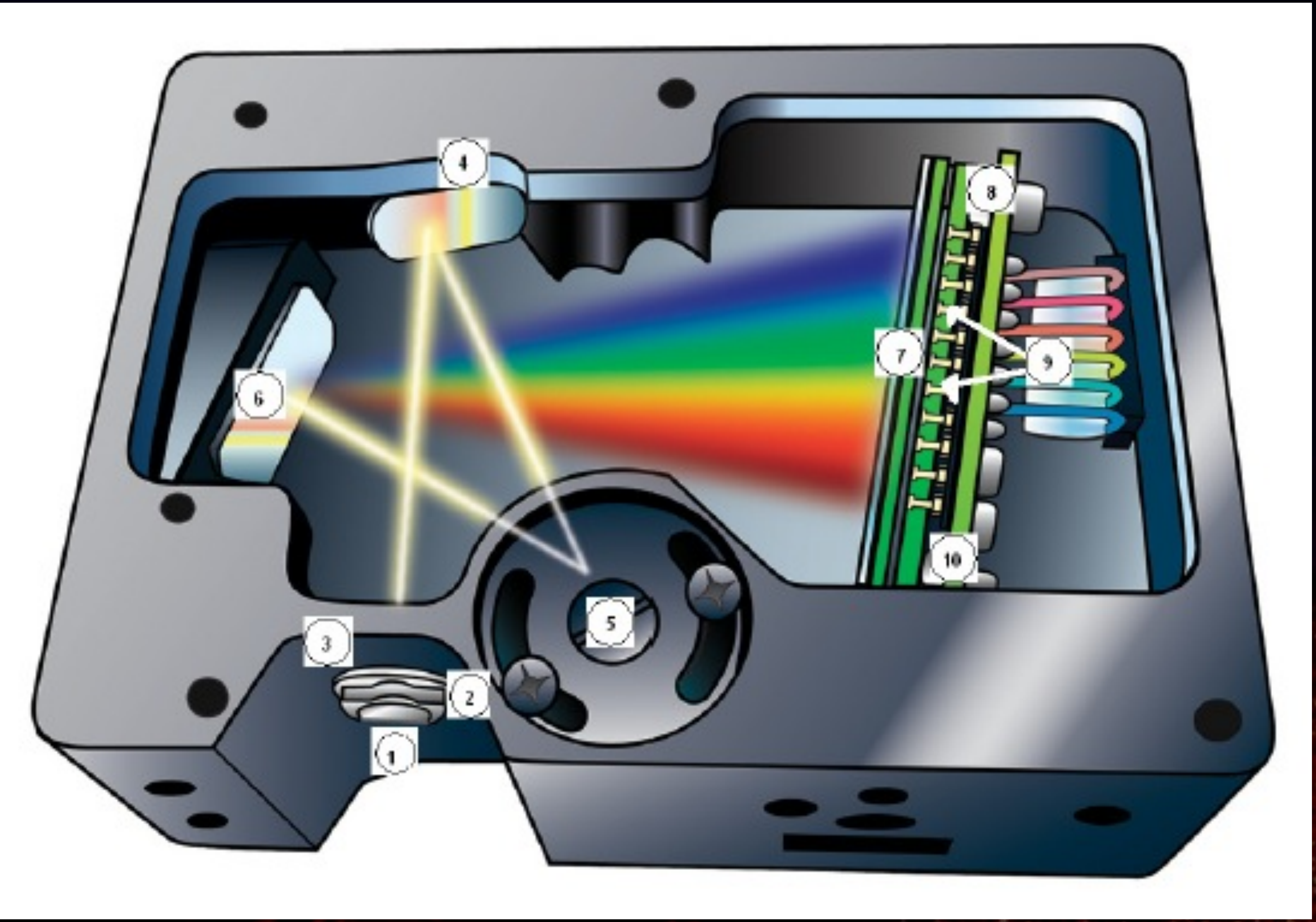

Helicopter-borne measurements of SO_2 flux

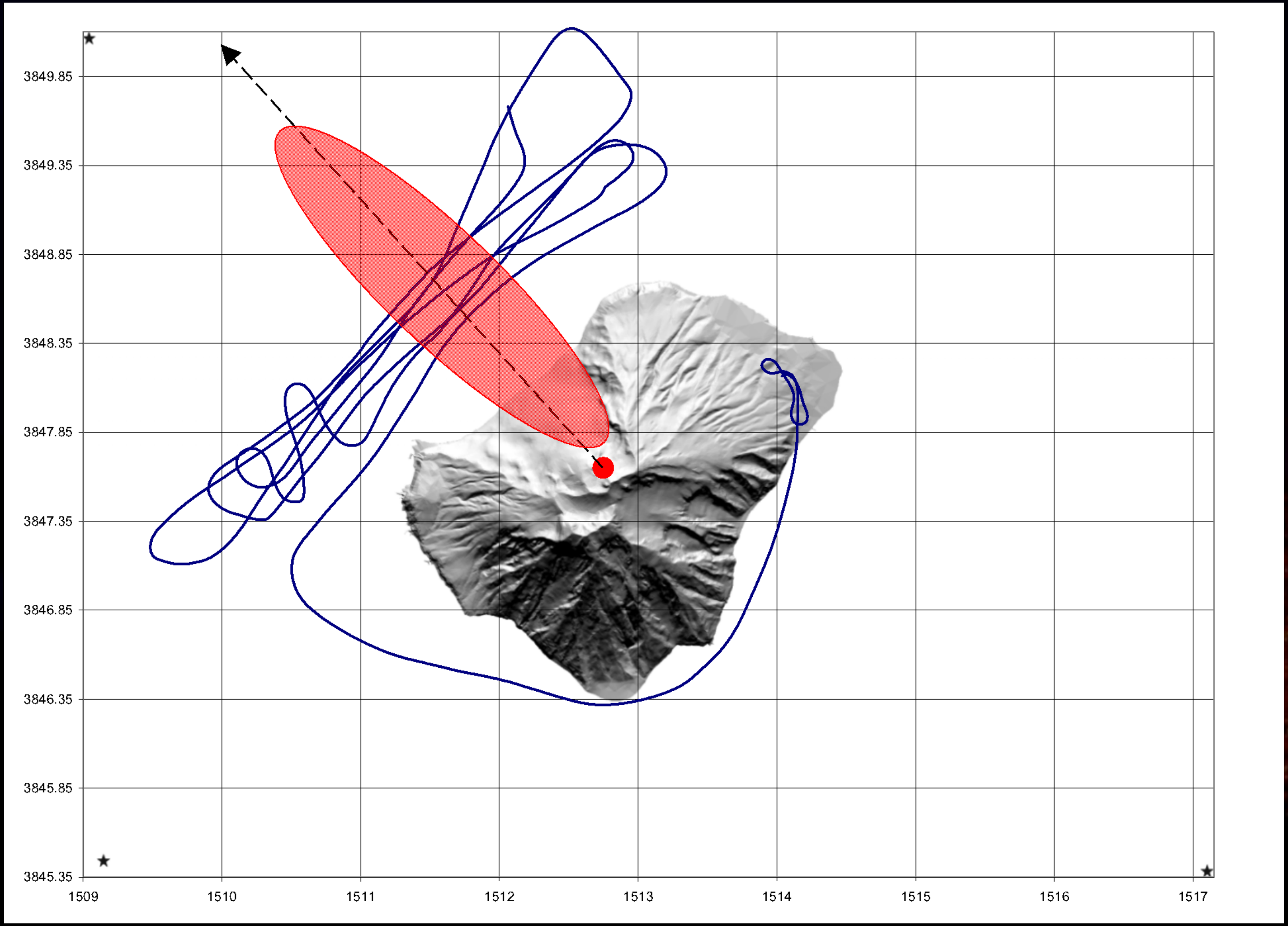

Helicopter-borne measurements of SO_2 flux

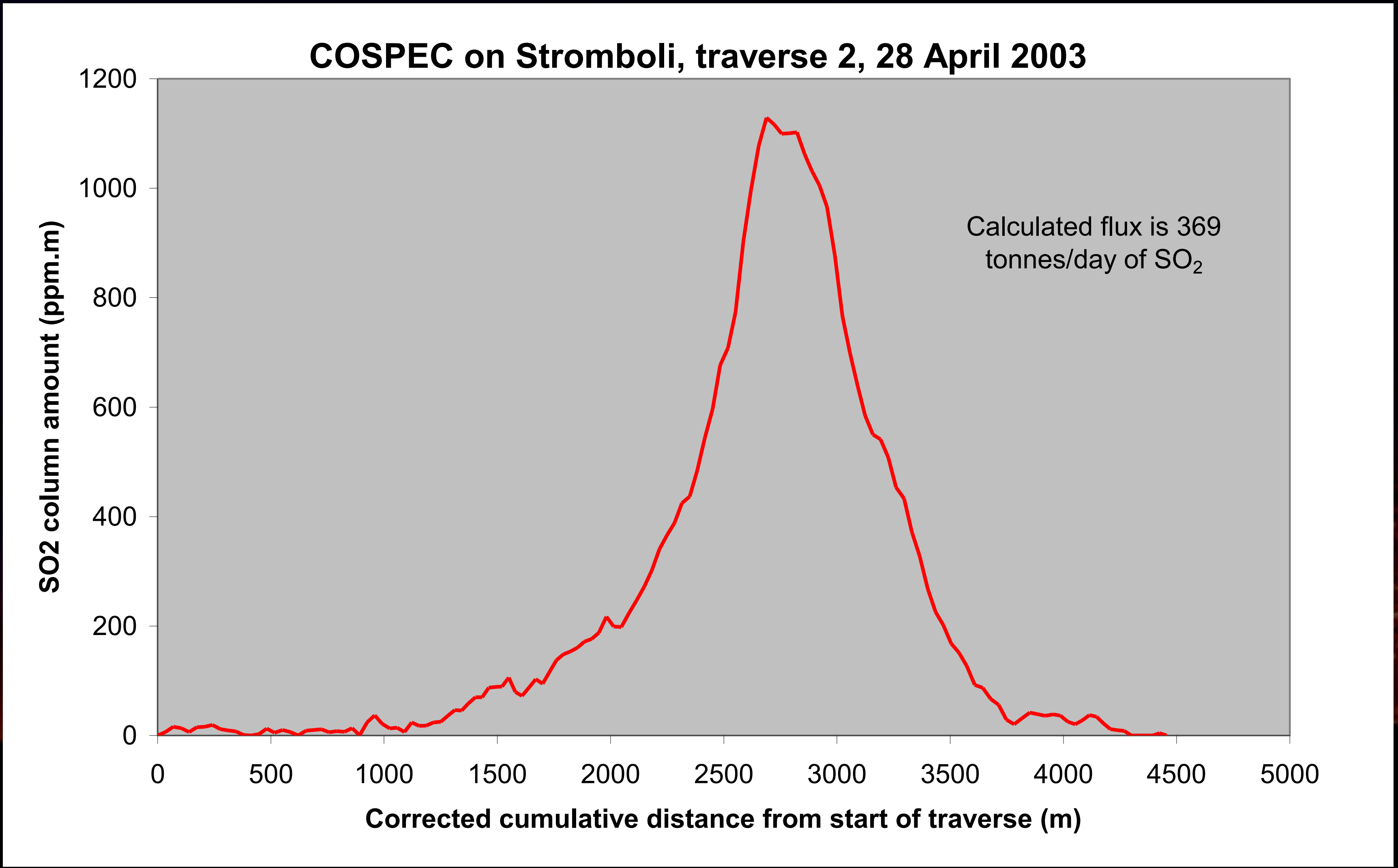

Fixed networks for SO2 flux monitoring

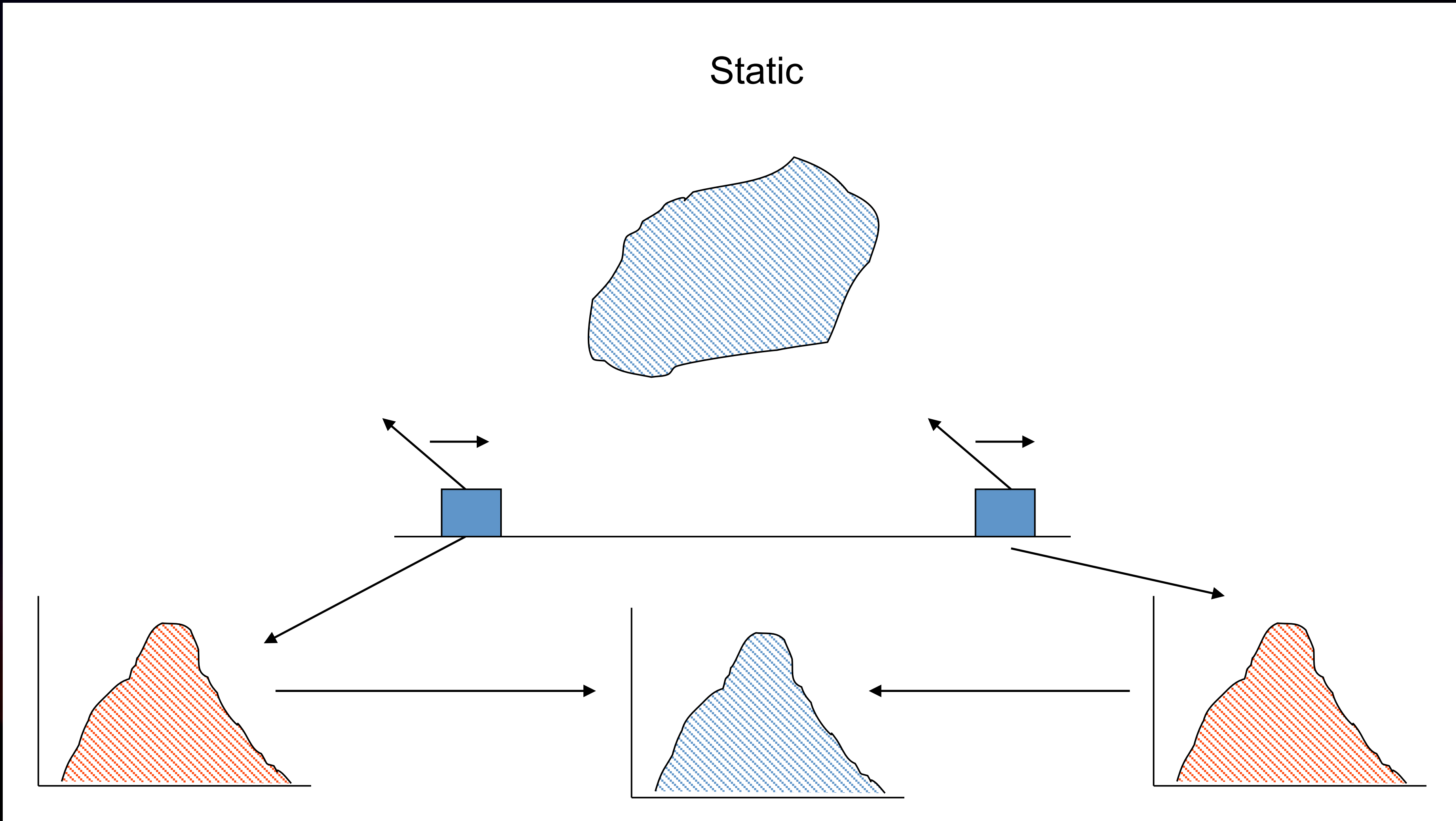

Fixed networks for SO2 flux monitoring: Etna

MiniDOAS networks: Montserrat

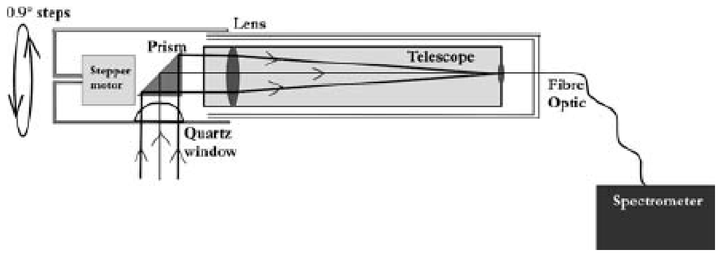

Fig. 2 The scanning and light collection devices used with both fixed scanning spectrometers at Soufrière Hills Volcano, Montserrat

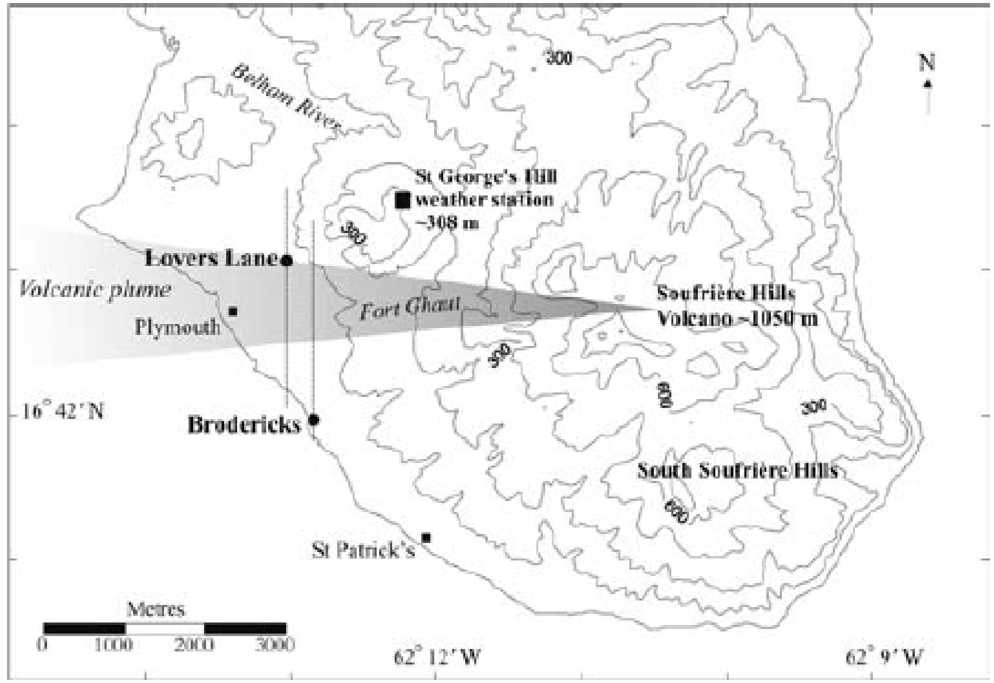

Fig. 1 Map of southern Montserrat to show the locations of the two fixed scanning spectrometers at Lovers Lane and Brodericks and the weather station, providing wind (plume) speeds. The plume is shown in its most common azimuthal position

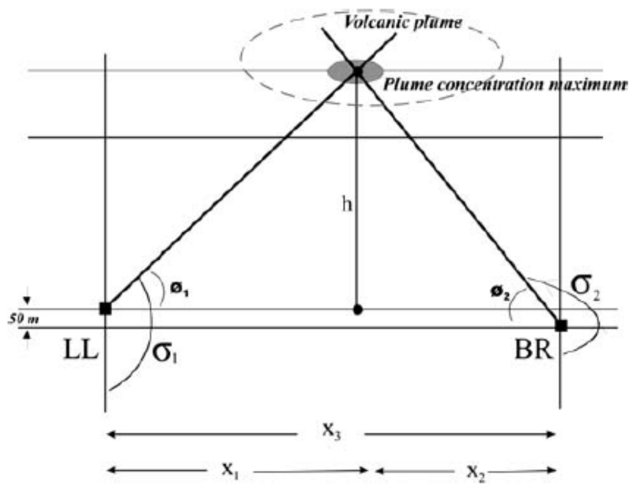

Fig. 6 Methodology for calculating plume height and position from the SO_2 concentration and angular data from the two fixed scanning spectrometers in Montserrat. Φ_1 and Φ_2 are calculated from Δ_1 and Δ_2, the scan angles for the peaks in SO_2 concentration measured during one revolution. Tan $\Phi_1=h/x_1$ and tan $\Phi_2=(h+50)/x_2$, where h is plume height. The height difference between the two spectrometers is 50 m (from GPS data) and x_1+x_2=2,800 m, the horizontal distance between them.

M. Edmonds · R. A. Herd · B. Galle · C. M. Oppenheimer

Bull Volcanol (2003) 65:578–586

Automated, high time-resolution measurements of SO_2 flux at Soufrière Hills Volcano, Montserrat

MiniDOAS networks: Stromboli

M.R. Burton et al. / Journal of Volcanology and Geothermal Research 182 (2009) 214–220

MiniDOAS networks: Stromboli

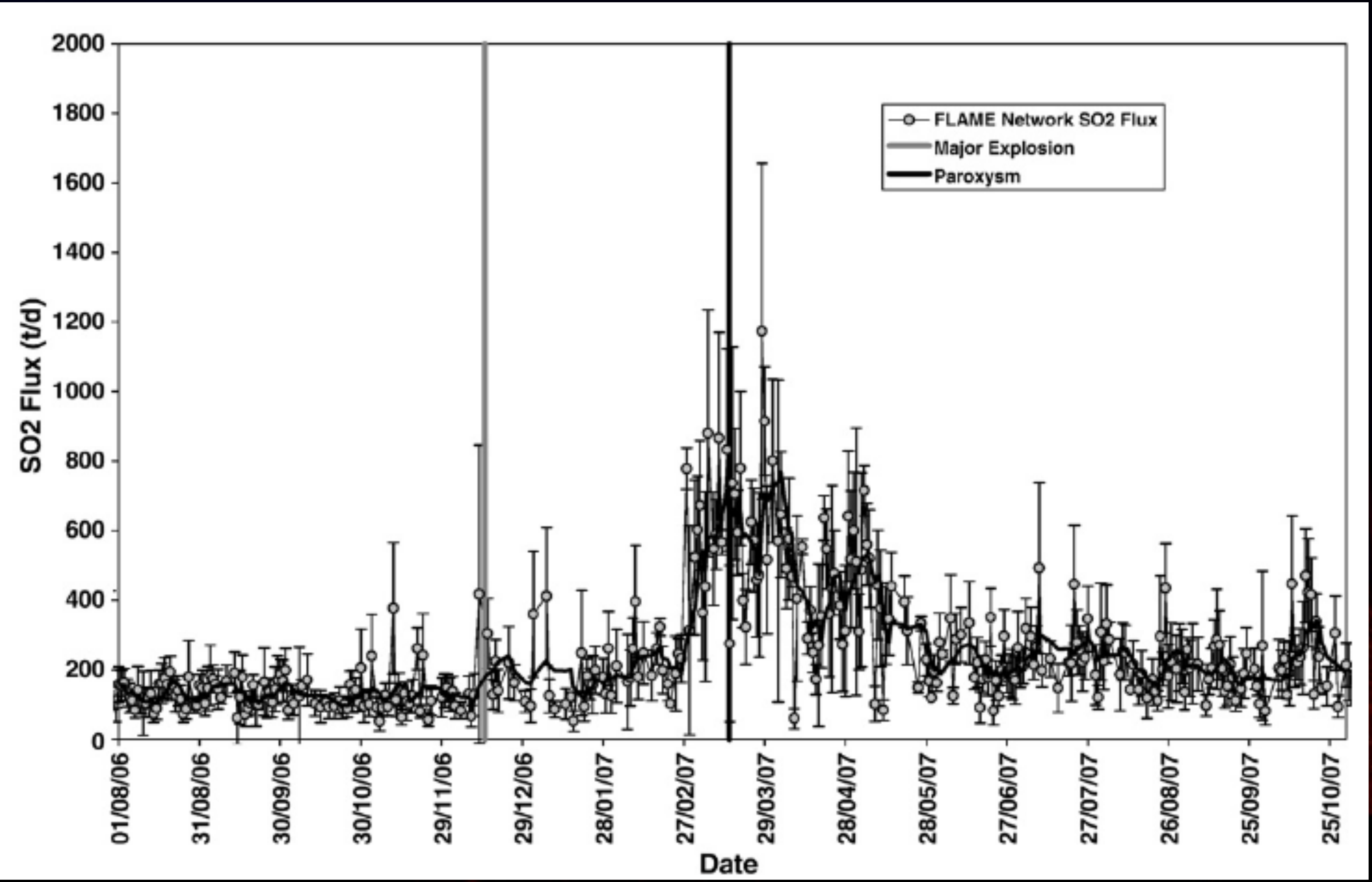

M.R. Burton et al. / Journal of Volcanology and Geothermal Research 182 (2009) 214–220

MiniDOAS networks: Stromboli and Etna

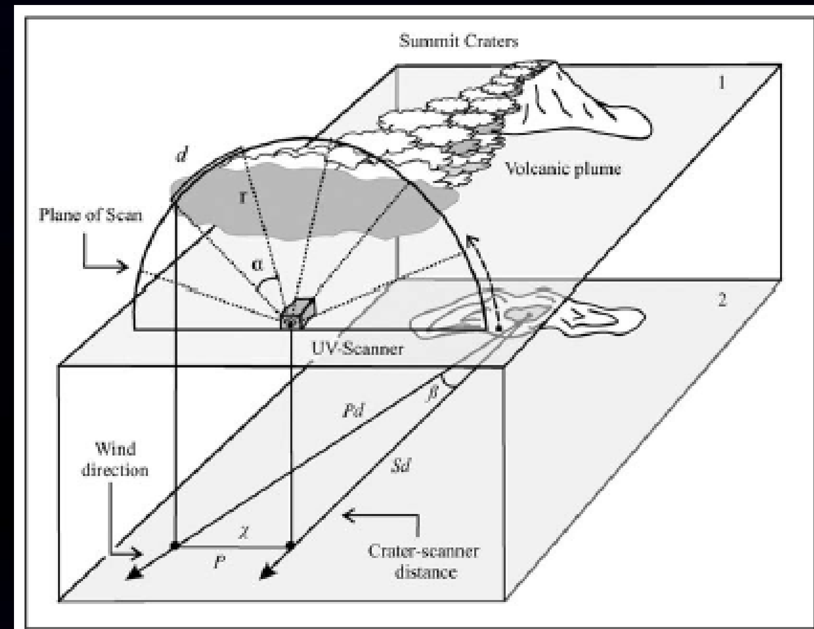

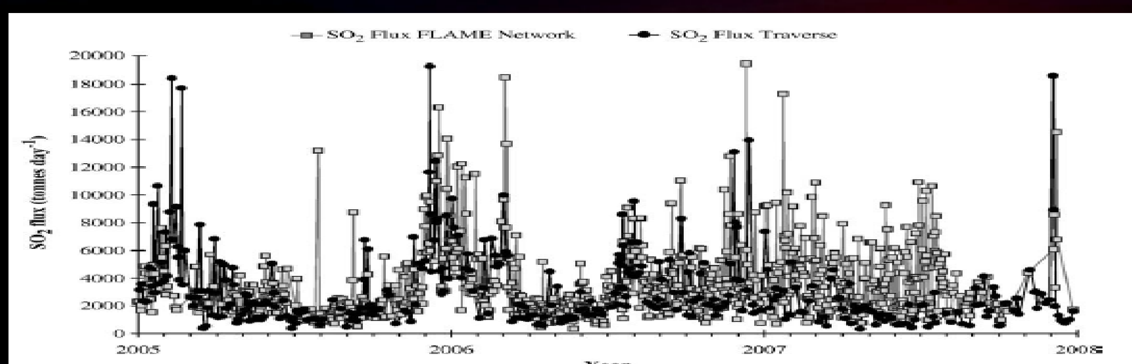

Journal of Volcanology and Geothermal Research 183 (2009) 76–83

Three-years of SO_2 flux measurements of Mt. Etna using an automated UV scanner array: Comparison with conventional traverses and uncertainties in flux retrieval

G.G. Salerno [a,b,*], M.R. Burton [a,c], C. Oppenheimer [b], T. Caltabiano [a], D. Randazzo [a], N. Bruno [a], V. Longo [a]

MiniDOAS networks: NOVAC

Network for Observation of Volcanic and Atmospheric Change (NOVAC)—A global network for volcanic gas monitoring: Network layout and instrument description

Bo Galle,[1] Mattias Johansson,[1] Claudia Rivera,[1] Yan Zhang,[1] Manne Kihlman,[2] Christoph Kern,[3] Thomas Lehmann,[3] Ulrich Platt,[3] Santiago Arellano,[1,4] and Silvana Hidalgo[4]

JOURNAL OF GEOPHYSICAL RESEARCH, VOL. 115, D05304, doi:10.1029/2009JD011823, 2010

MiniDOAS networks: NOVAC

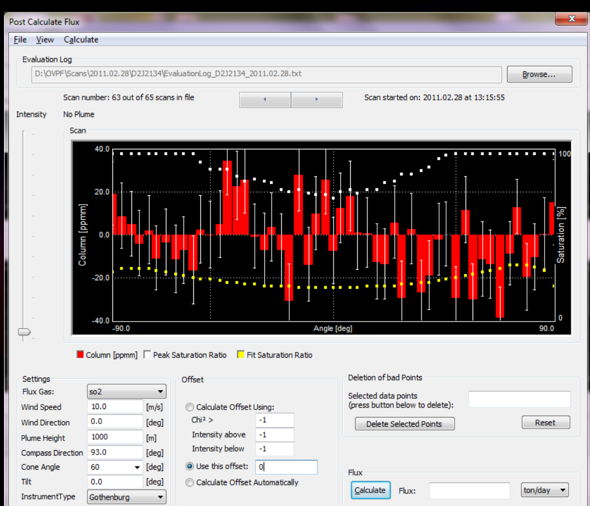

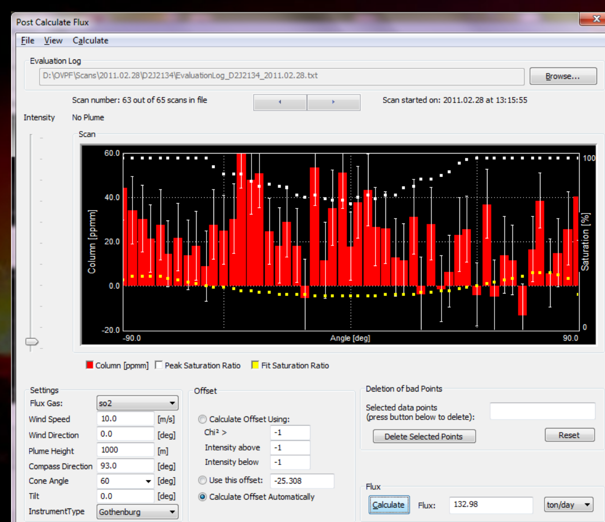

Network for Observation of Volcanic and Atmospheric Change (NOVAC)—A global network for volcanic gas monitoring: Network layout and instrument description

Bo Galle,[1] Mattias Johansson,[1] Claudia Rivera,[1] Yan Zhang,[1] Manne Kihlman,[2] Christoph Kern,[3] Thomas Lehmann,[3] Ulrich Platt,[3] Santiago Arellano,[1,4] and Silvana Hidalgo[4]

JOURNAL OF GEOPHYSICAL RESEARCH, VOL. 115, D05304, doi:10.1029/2009JD011823, 2010

MultiGas + DOAS Networks = CO_2 & SO_2 Flux monitoring

CO_2/SO_2 ratio increase can be produced by increase in CO_2 or decrease in SO_2

Fluxes allow unique interpretation of the gas variations

This reveals degassing from different depths in the Stromboli system

Empirical data leads to new models of eruptive processes

MultiGas + DOAS Networks: Stromboli

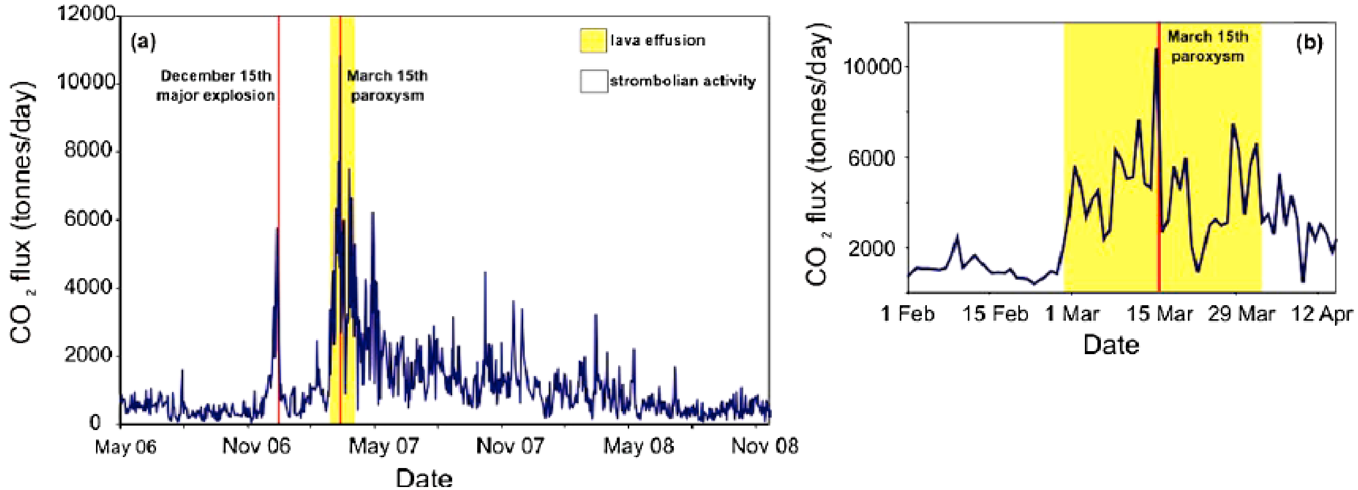

Figure 2. (a) Daily averages of CO_2 fluxes (in tonnes per day) from Stromboli's summit crater plume, from May 2006 to November 2008. (b) A detail of the 1 February to 15 April period. Typical errors for CO_2 fluxes are ~39%.

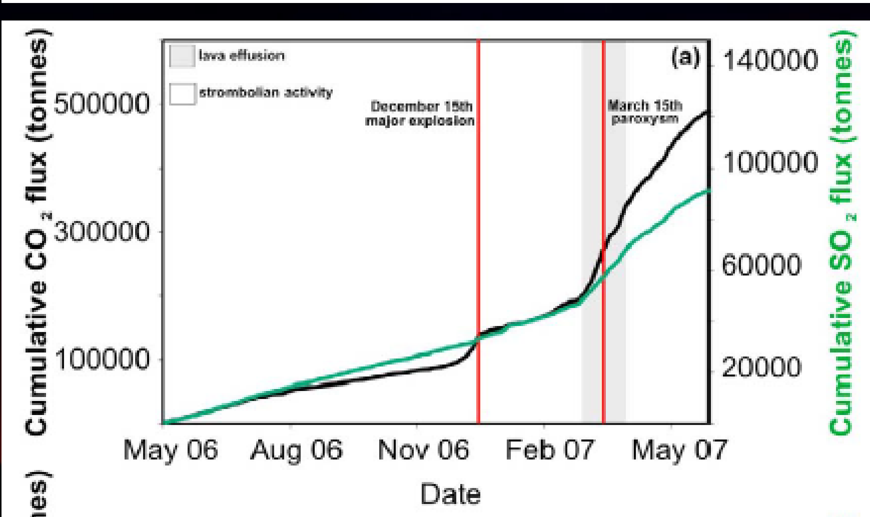

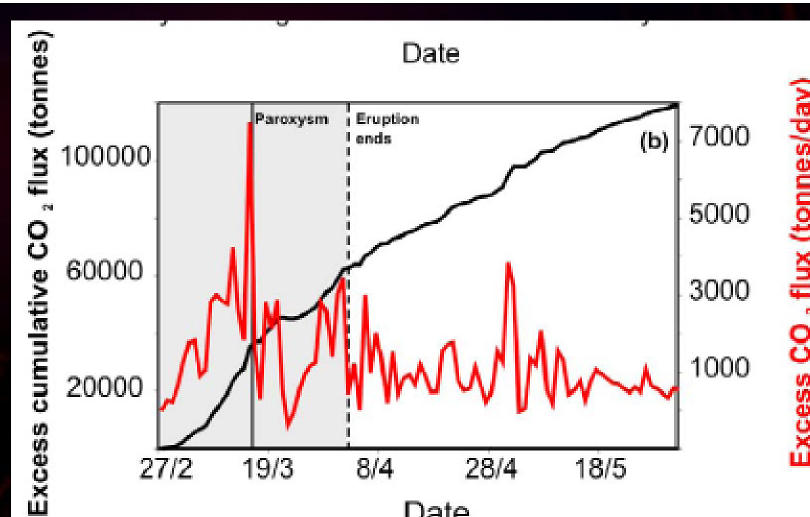

Unusually large magmatic CO_2 gas emissions prior to a basaltic paroxysm

Alessandro Aiuppa,[1,2] Mike Burton,[3] Tommaso Caltabiano,[4] Gaetano Giudice,[2] Sergio Guerrieri,[2] Marco Liuzzo,[2] Filippo Murè,[4] and Giuseppe Salerno[4]

GEOPHYSICAL RESEARCH LETTERS, VOL. 37, L17303, doi:10.1029/2010GL043837, 2010

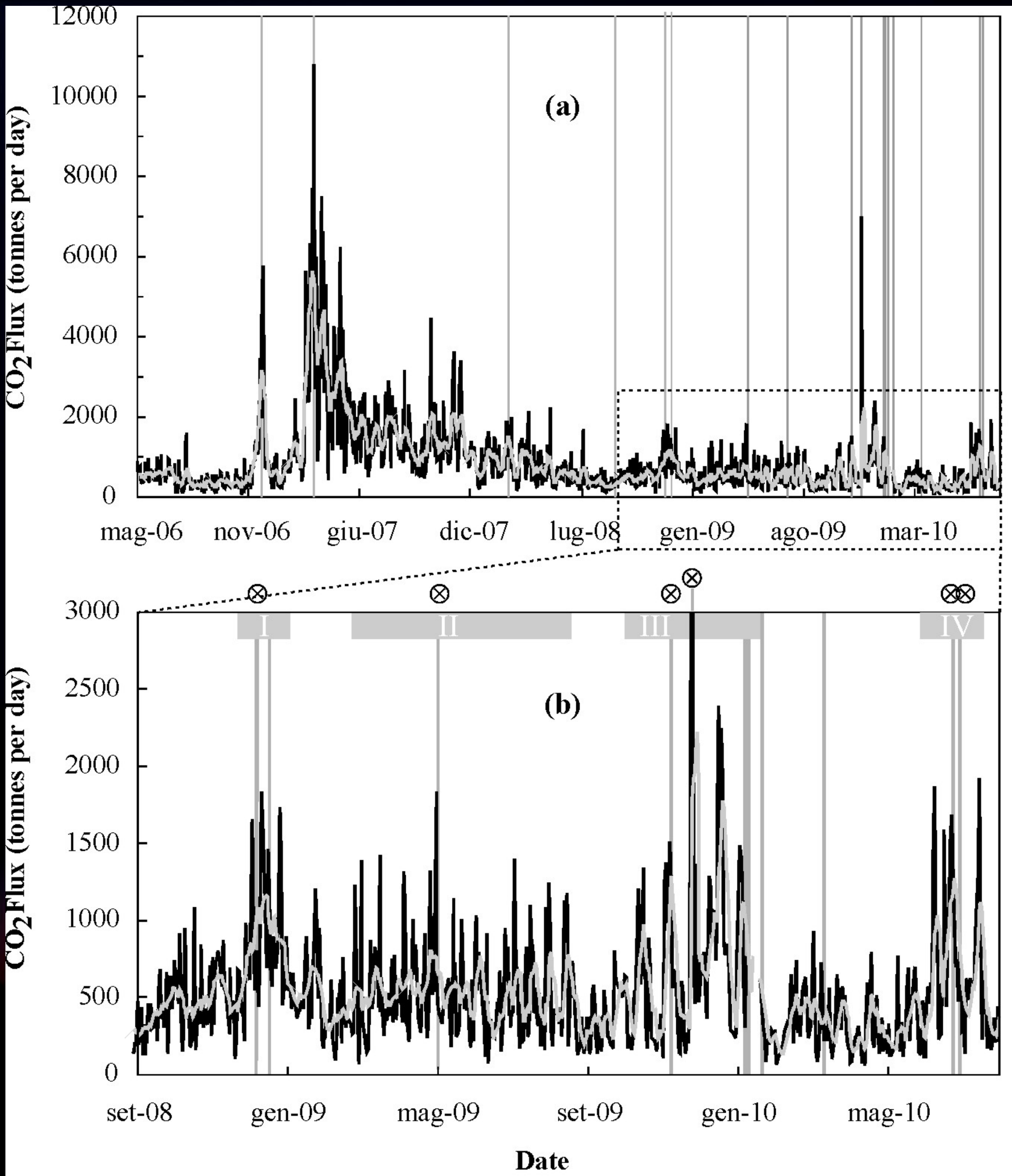

Aiuppa et al., Solid Earth, 2011

CO2 fluxes from MultiGas+DOAS

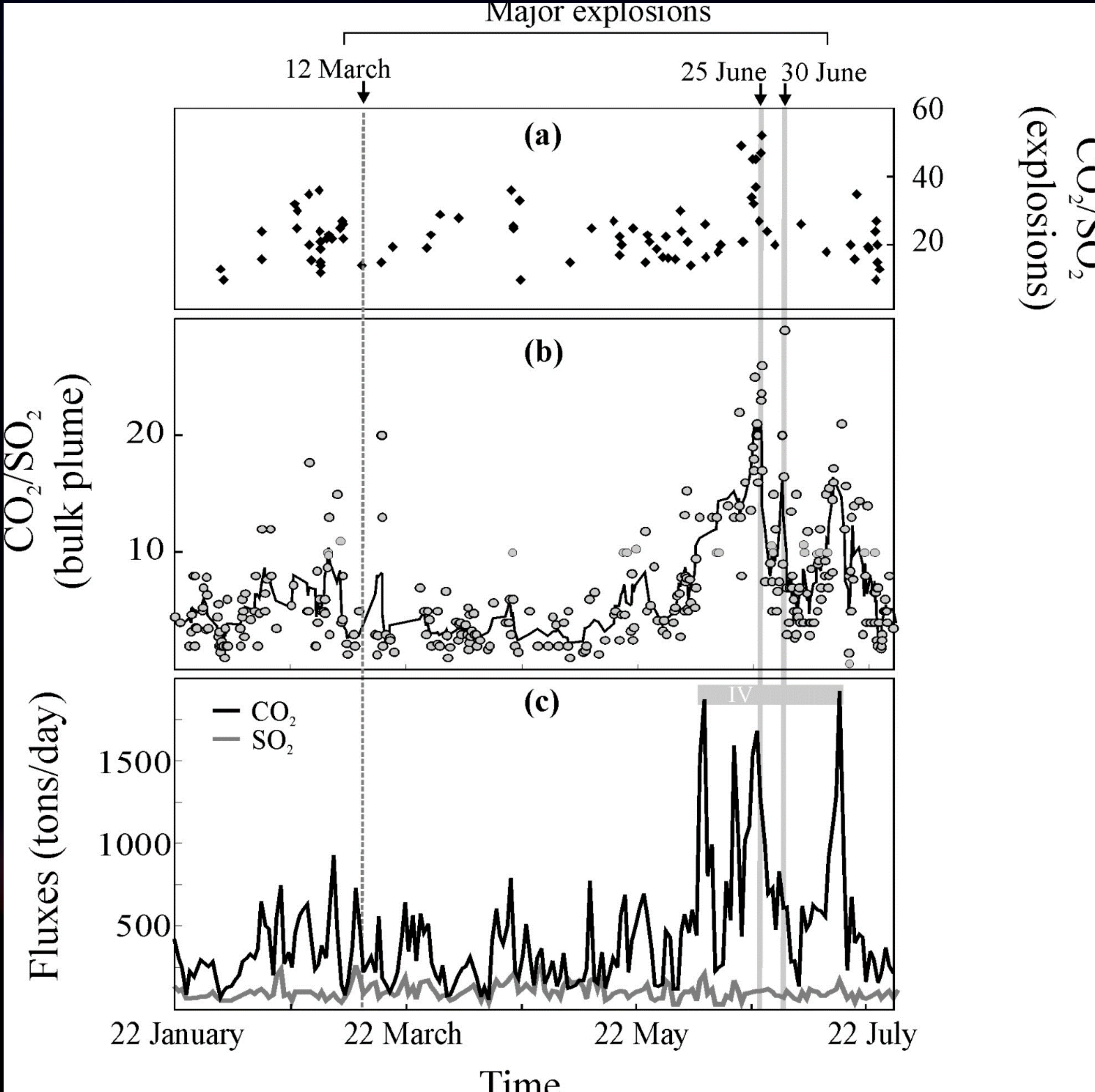

Aiuppa et al., Solid Earth, 2011

CO2 fluxes from MultiGas+DOAS

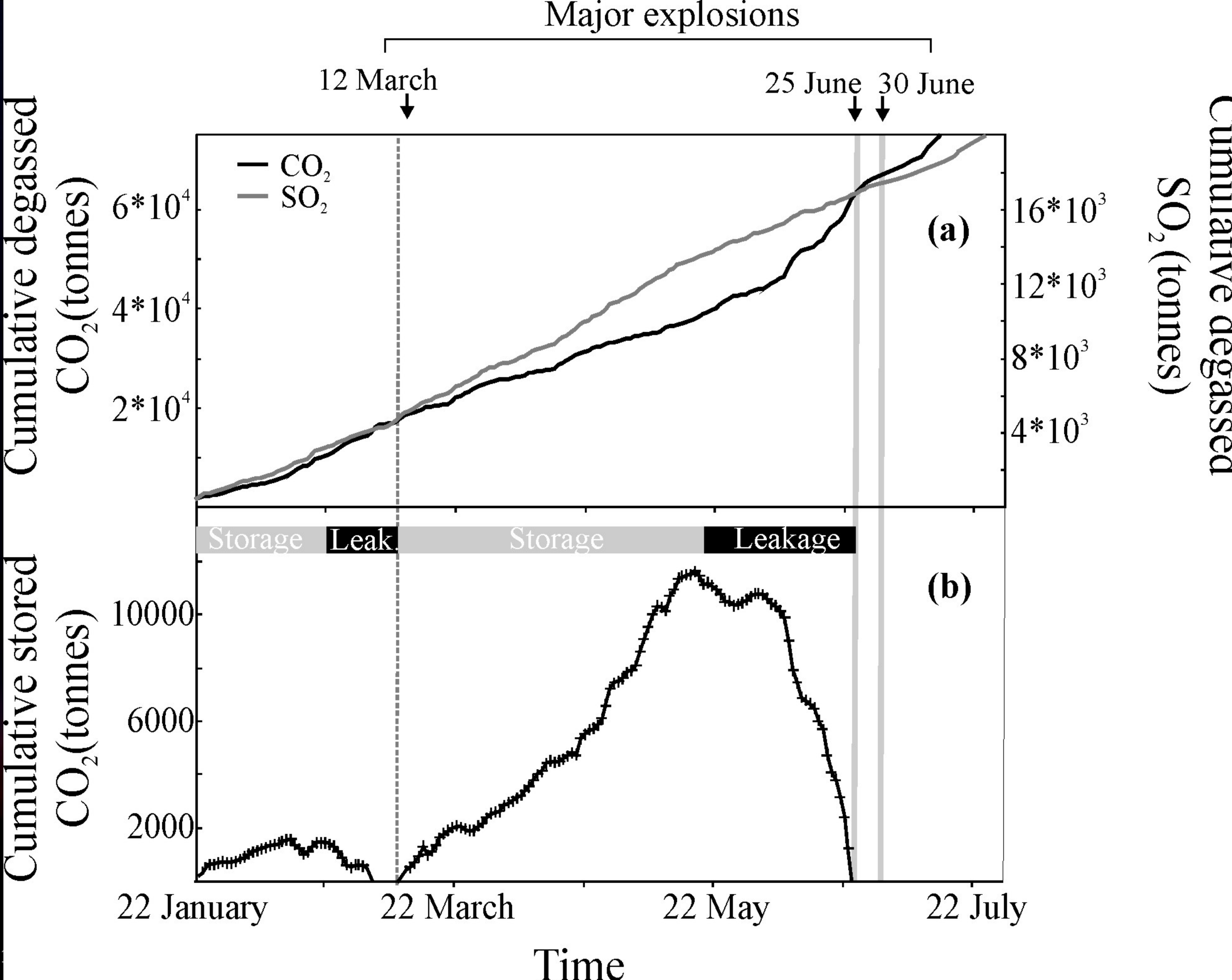

Major explosions
12 March
25 June
30 June
CO2
SO2
(a)
(b)
Cumulative degassed CO2(tonnes)
Cumulative degassed SO2(tonnes)
6*10^4
4*10^4
2*10^4
16*10^3
12*10^3
8*10^3
4*10^3
Storage
Leak.
Storage
Leakage
Cumulative stored CO2(tonnes)
10000
6000
2000
22 January
22 March
22 May
22 July
Time

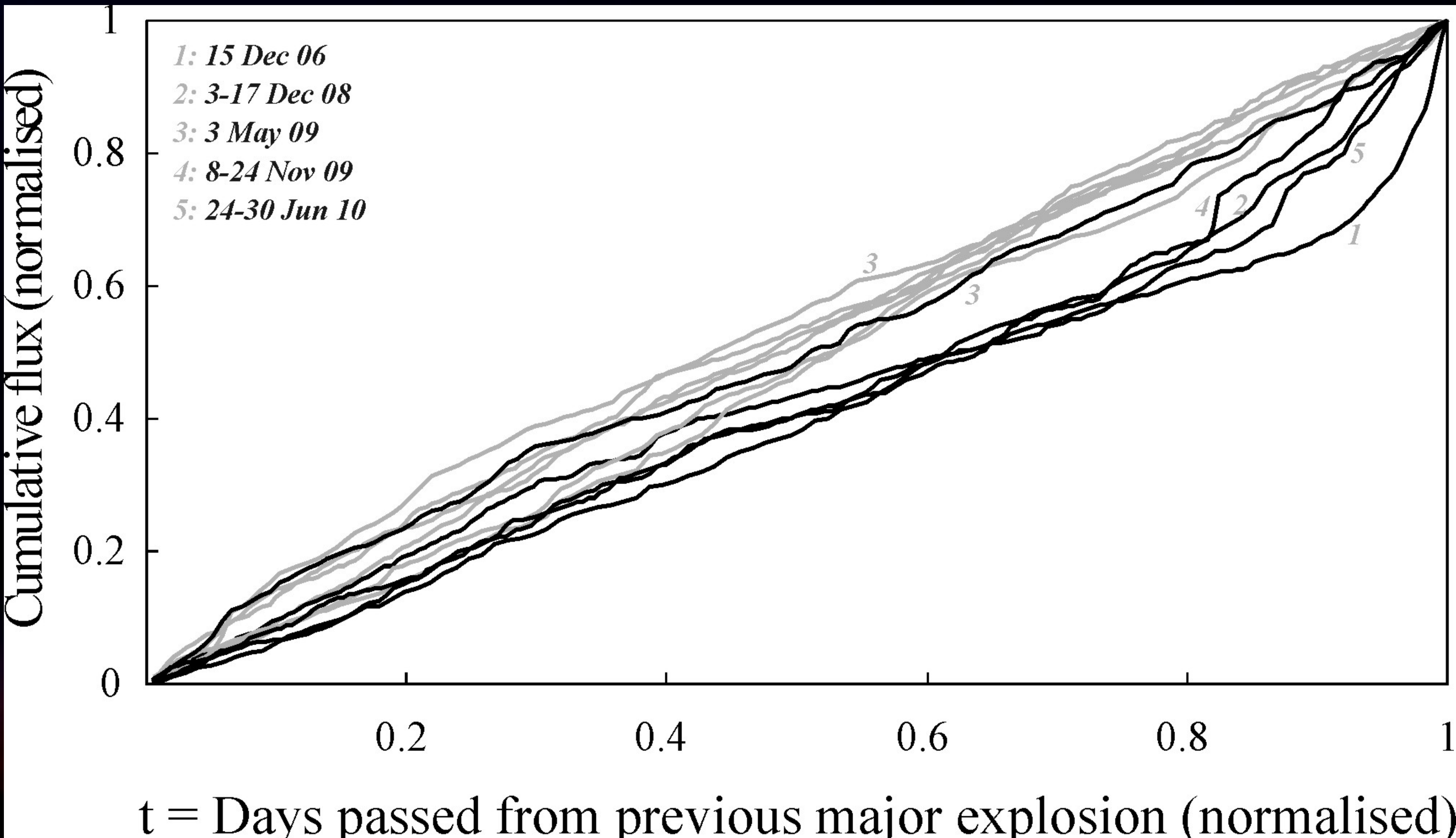
1: 15 Dec 06
2: 3-17 Dec 08
3: 3 May 09
4: 8-24 Nov 09
5: 24-30 Jun 10
Cumulative flux (normalised)
0
0.2
0.4
0.6
0.8
1
0.2
0.4
0.6
0.8
1
t = Days passed from previous major explosion (normalised)
3
3
4
2
5
1

The SO2 Camera

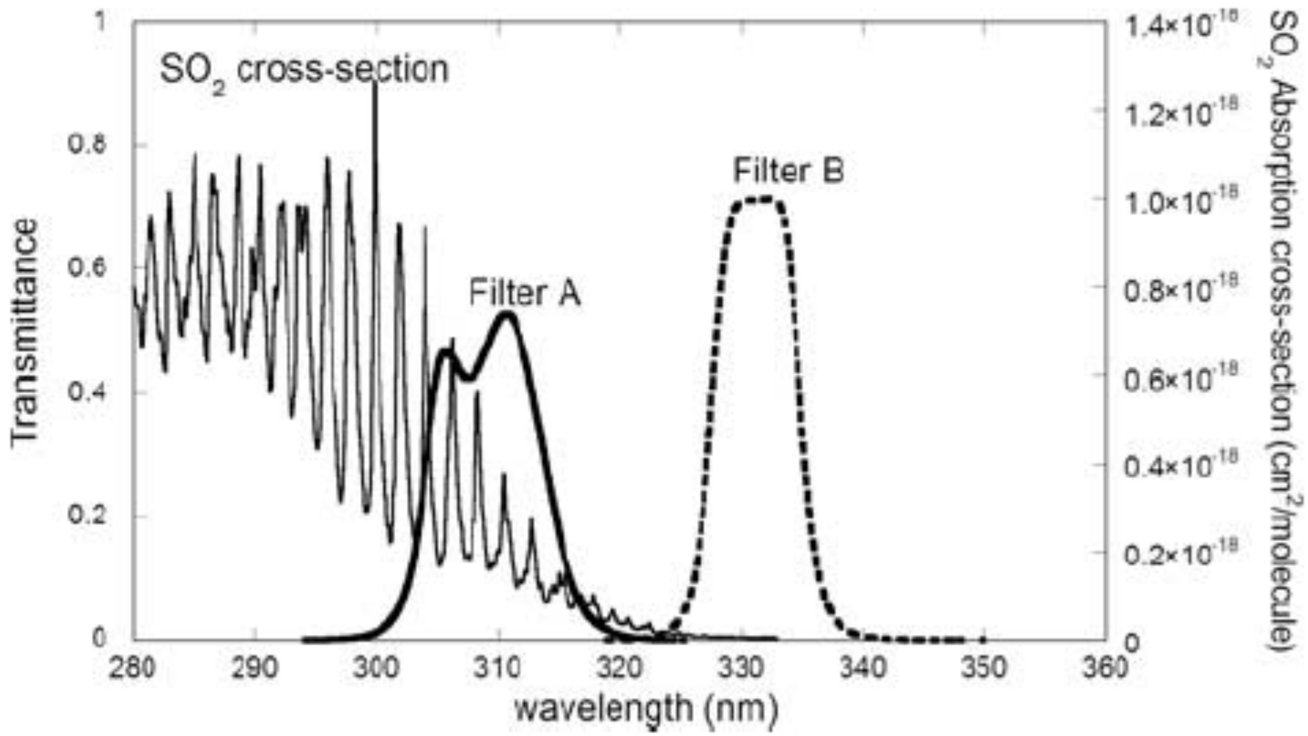

Figure 1. Transmittance of the filters A and B with SO_2 absorption cross-section between 280 and 360 nm.

GEOPHYSICAL RESEARCH LETTERS, VOL. 33, L24804, doi:10.1029/2006GL027916, 2006

The SO_2 camera: A simple, fast and cheap method for ground-based imaging of SO_2 in volcanic plumes

Toshiya Mori[1] and Mike Burton[2]

The SO2 Camera

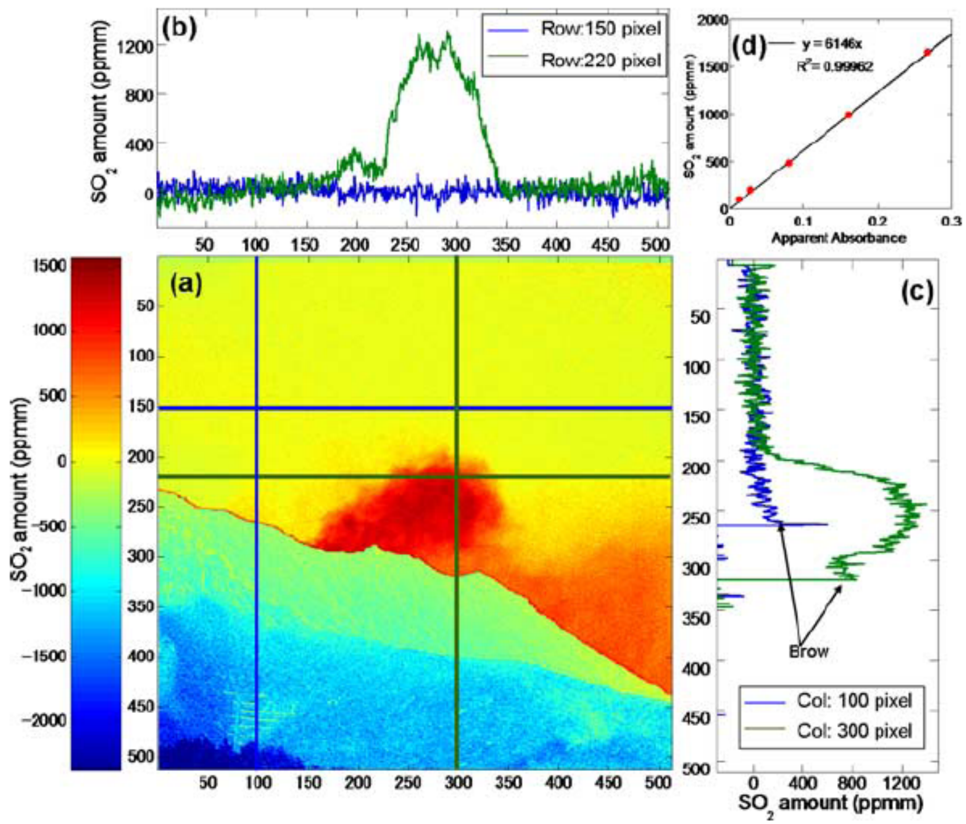

Figure 3. (a) SO_2 column amount image of the volcanic plume at 14:09:54. The scale on the left is in ppm.m of SO_2. (b) Horizontal distribution of the SO_2 column amount at 150 (blue) and 220 (green) row pixels. (c) Vertical SO_2 column amount at 100 (blue) and 300 (green) column pixels. (d) The result of a calibration of the SO_2 camera using calibration cells.

The SO2 Camera

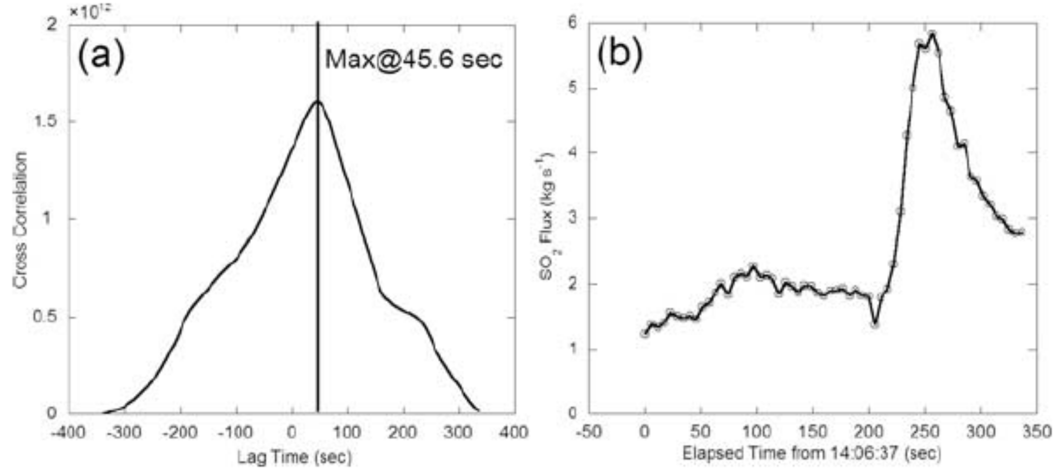

Figure 4. (a) Cross-correlation of temporal variations in integrated profiles calculated between the 300th and 400th vertical columns. The derived time lag was 45.6 s over a distance of ~244 m (100 pixels at 2.44 m width each), resulting in a wind speed of 5.4 ms^{-1}. (b) Temporal variations of SO_2 flux obtained from profiles of the 400th vertical column. Note the sudden increase related to a puff of gas.

4 of 5

The SO2 Camera: Advantages

- Resolves two main sources of error in fixed networks , plume velocity and plume height

- Allows high frequency sampling rates, comparison with geophysical parameters

The SO2 Camera: Disadvantages

- More complex data analysis compared with older methods
- Large data rates (up to 200 MB / minute)
- Not quite ready for use as an automatic monitoring tool

SO_2 Camera: Stromboli Explosions

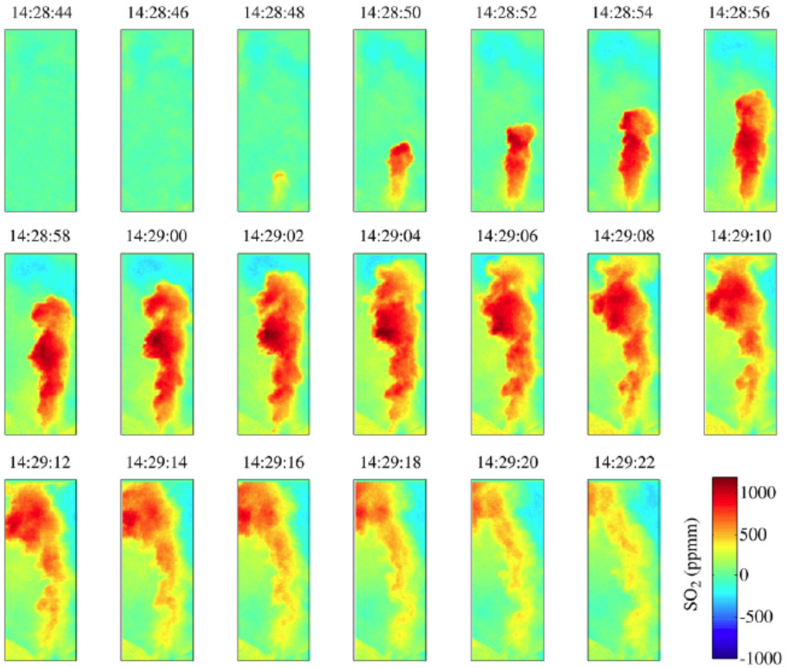

Fig. 3. Time-sequence of SO_2 column amount images of a single hornito eruption that occurred at 14:28:48. Images were collected every 2 s starting at 14:28:44. Each pixel has a equivalent size at the distance to the explosive plume (~650 m) of 0.5 m × 0.5 m. The images are 150 × 380 pixels corresponding to75 m × 190 m at the plume.

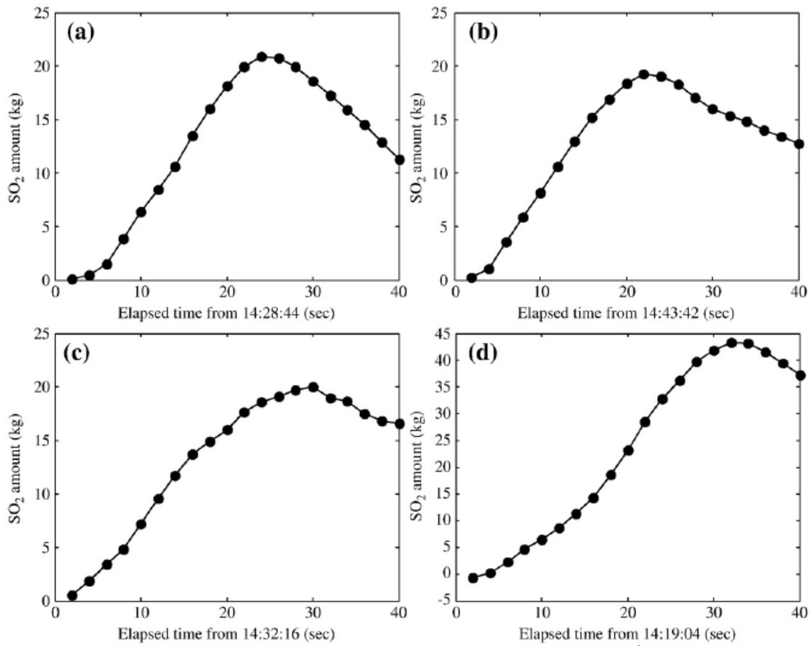

Fig. 4. SO_2 mass amount time series for 4 hornito eruptions observed on Oct. 3, 2006.

Quantification of the gas mass emitted during single explosions on Stromboli with the SO_2 imaging camera

Toshiya Mori [a], Mike Burton [b,*]

Journal of Volcanology and Geothermal Research 188 (2009) 395–400

SO_2 Camera: Santiaguito Explosions

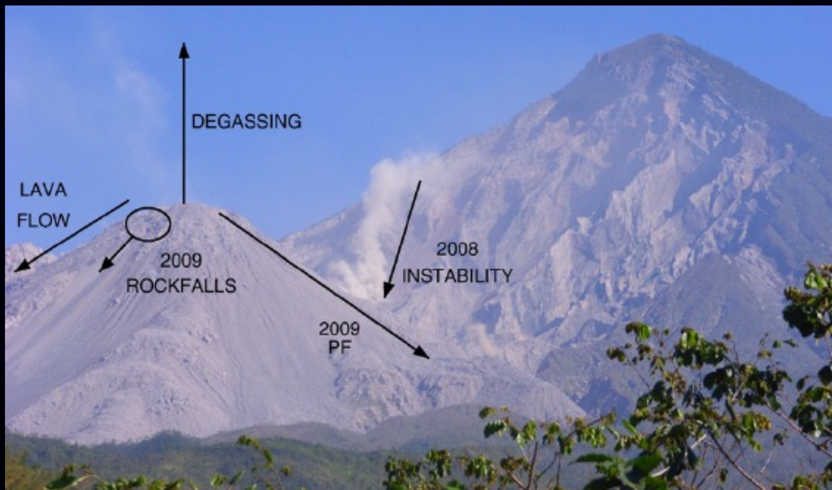

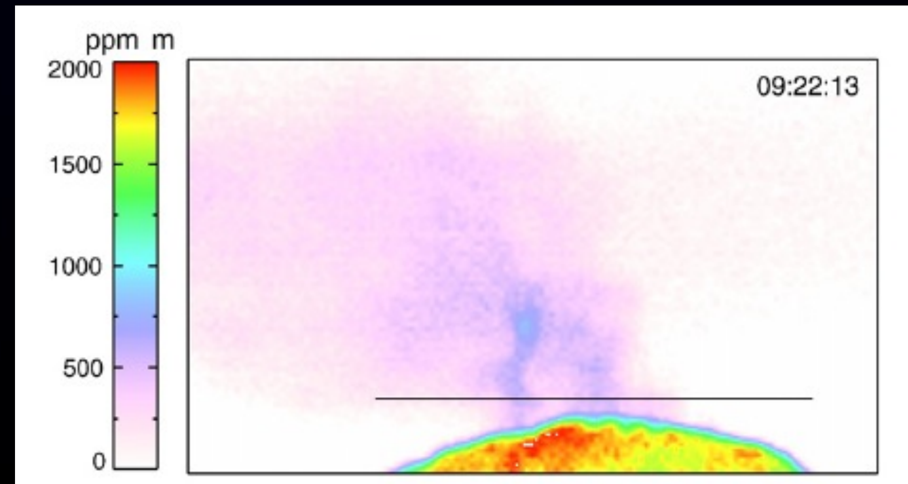

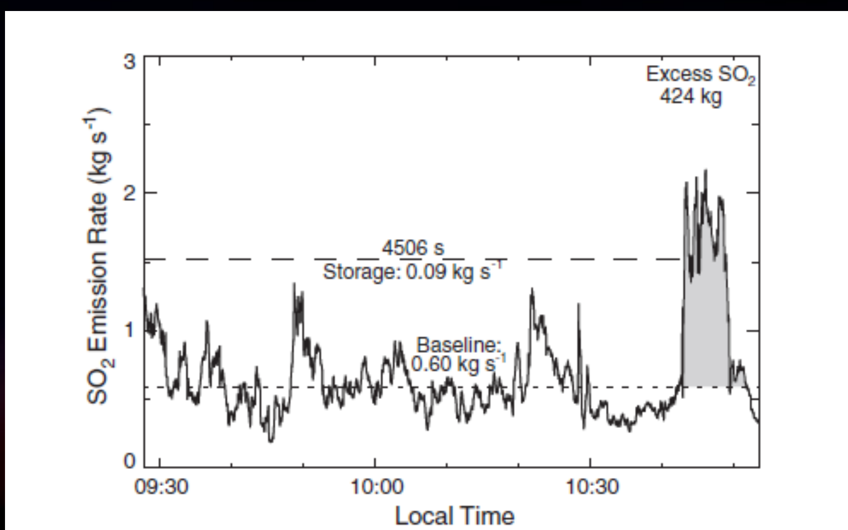

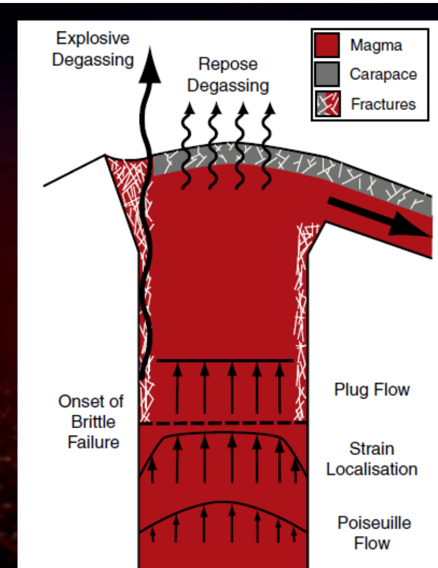

Degassing processes during lava dome growth: Insights from Santiaguito lava dome, Guatemala

A.S.P. Holland et al. / Journal of Volcanology and Geothermal Research 202 (2011) 153–166

A.S. Peter Holland [a,*], I. Matthew Watson [a], Jeremy C. Phillips [a], Luca Caricchi [a], Marika P. Dalton [b]

SO_2 Camera: Fuego VLP events

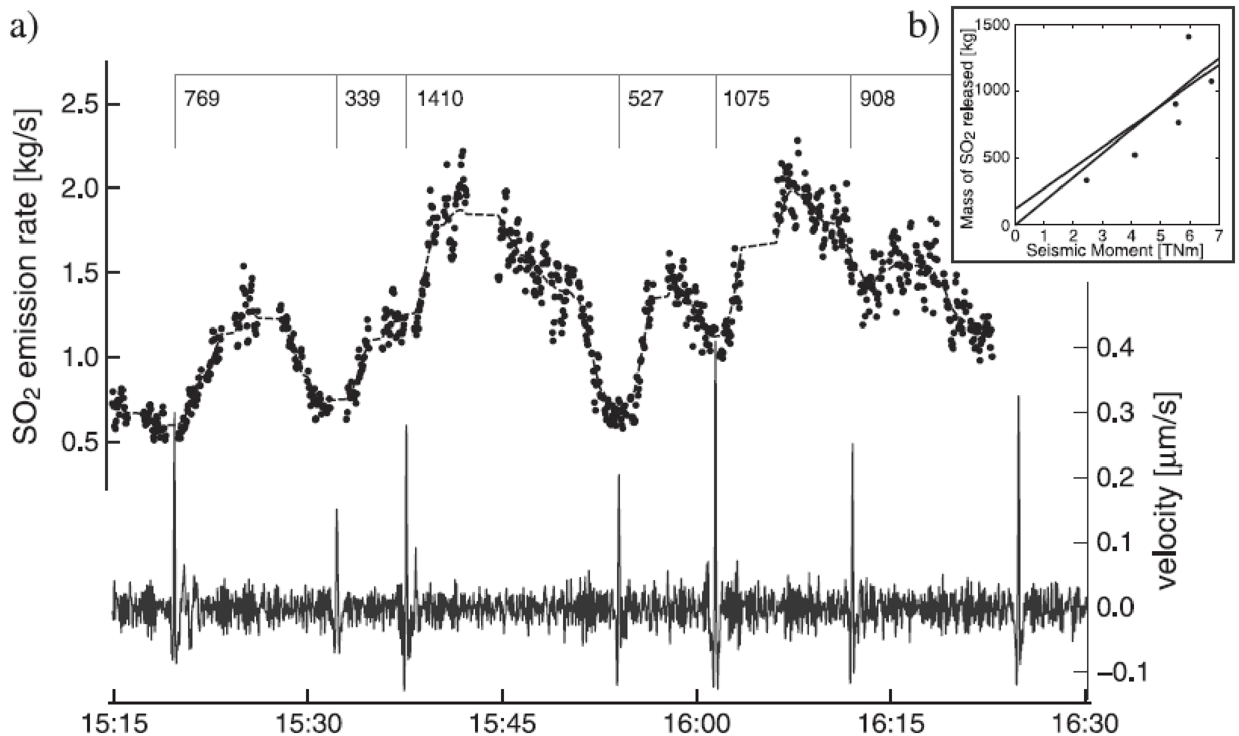

Figure 4. Temporal correlation between Type 3 VLP events (solid line in a) and SO_2 emission rate (dots in a) plotted for about 90 min on 15 January 2008. Masses computed for each of the six events are listed

WAITE ET AL.: VLP EVENTS AND ERUPTION VARIABILITY

Scattered sunlight UV measurements

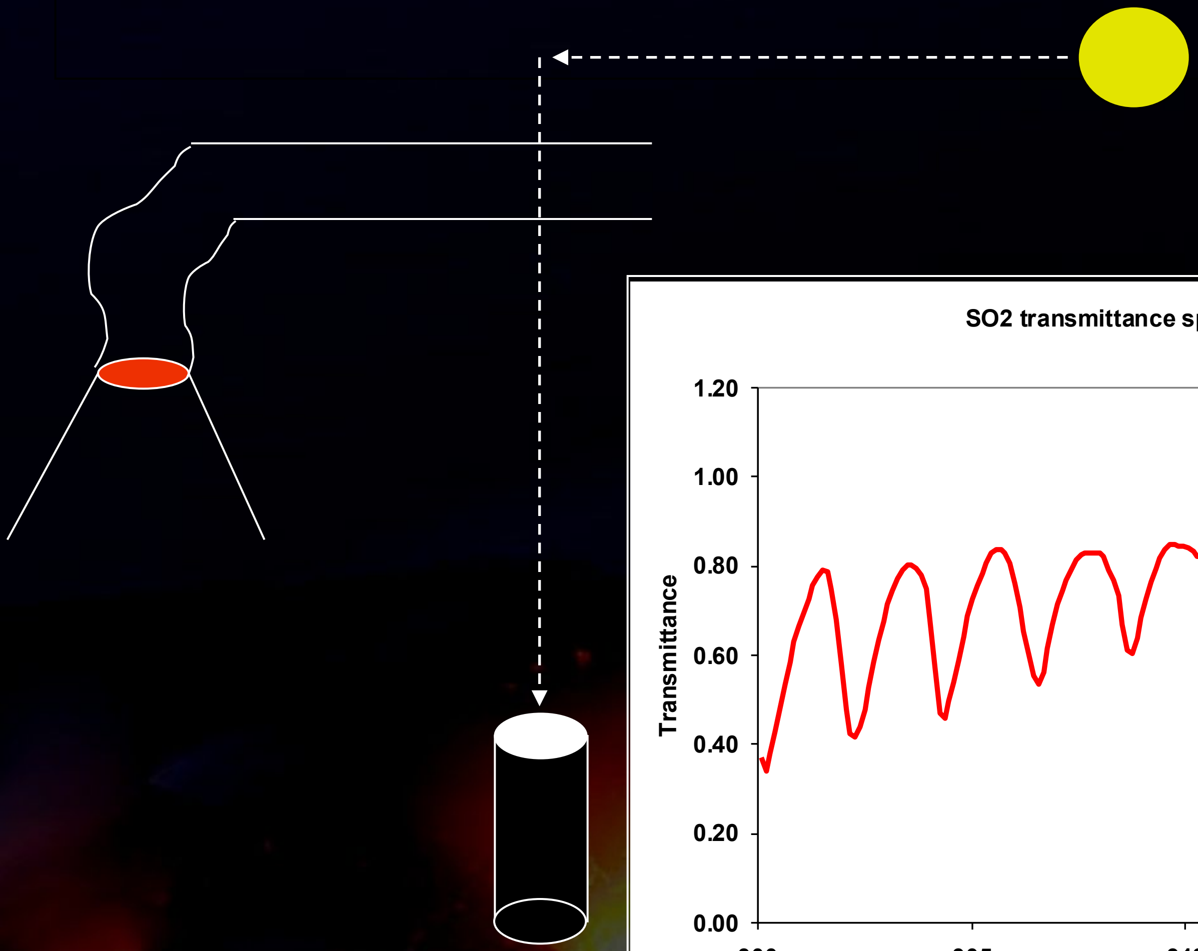

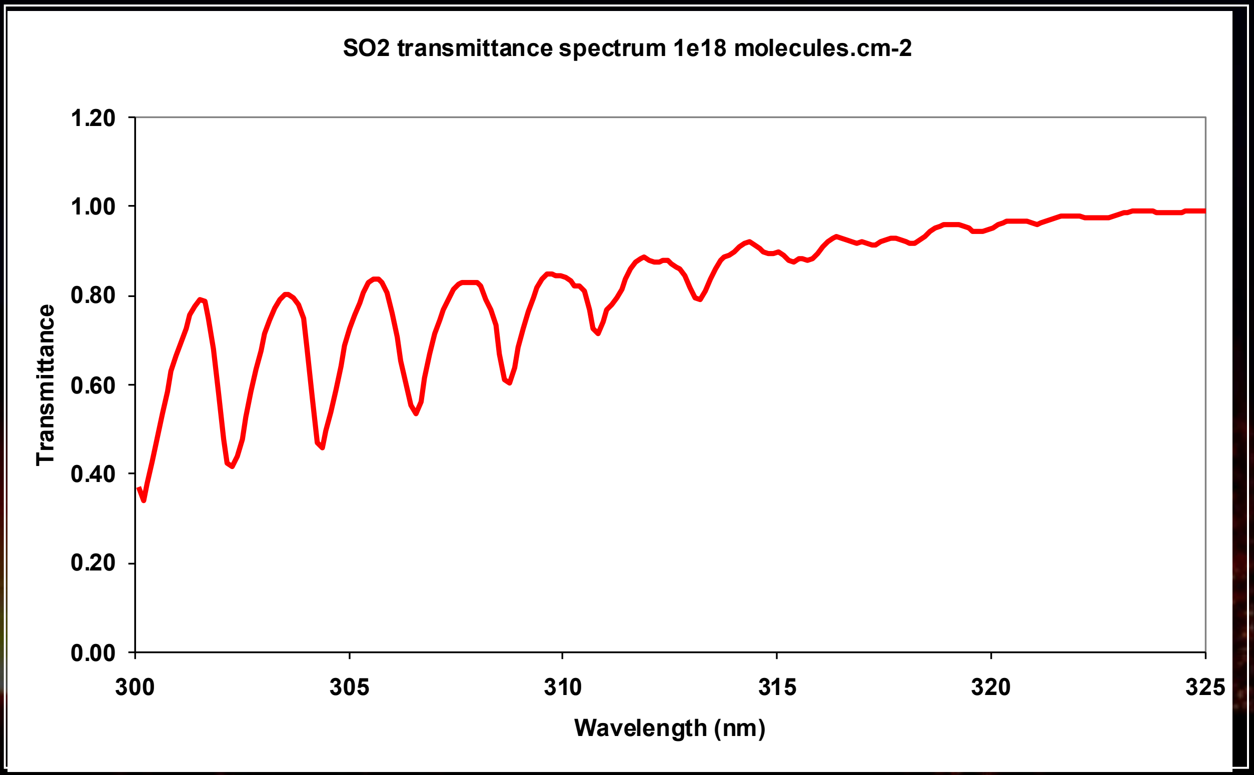

Light Dilution

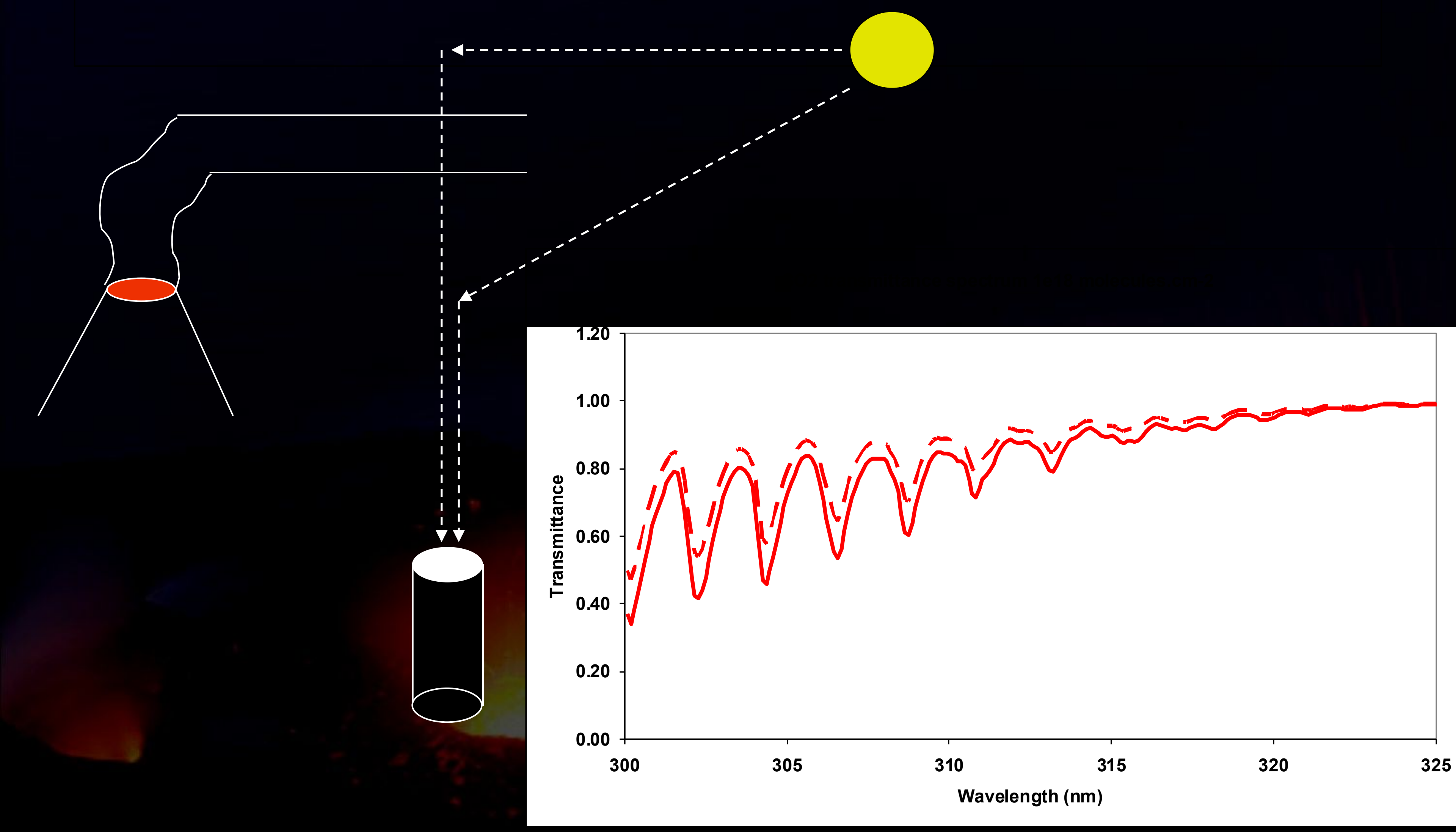

Some potential magma tectonic interaction

Melt Inclusions and Quiescent Degassing

We can determine the minimum mass of magma required to produce an observed gas flux.

• Typical original S contents of Etna basalt is 0.32 wt%

Melt Inclusions and Quiescent Degassing

We can determine the minimum mass of magma required to produce an observed gas flux.

- Typical original S contents of Etna basalt is 0.32 wt%
- Typical final S content of erupted Etna basalt is 0.005 wt%

Melt Inclusions and Quiescent Degassing

We can determine the minimum mass of magma required to produce an observed gas flux.

- Typical original S contents of Etna basalt is 0.32 wt%
- Typical final S content of erupted Etna basalt is 0.005 wt%
- To first approximation all S is lost during ascent to the surface

Mass Balance from S and SO2

Typical SO_2 fluxes from Etna are 3000 tonnes of SO2 per day (0.6×10^{12} g/yr)

It’s a lot. Typical of a large unfiltered coal-burning power station.

Indeed the total SO_2 emission from volcanoes (while very poorly constrained) is estimated to be about 10% of that produced by human activities

7.5–10.5×1012 g/yr S, amounting to 10–15% of the annual anthropogenic sulfur output (70×1012 g/yr S during the decade 1981–1990) Halmer et al., 2002

Note that Etna is 5% of global volcanic S emissions -> suggests underestimate

Mass Balance from S and SO_2

Typical SO_2 fluxes from Etna are 3000 tonnes of SO_2 per day

How much magma is needed to produce this gas flux?

SO_2 flux of 3000 t/d = S flux of 1500 t/d (SO$_2$ MW=64g, S AW=32g)

S content of Etnean magma is 0.32 wt%

1500 tonnes = 1.5 million kg of S, divided by 0.32 wt% gives the magma mass:

4.7×10^9 kg of magma required per day

Typical magma density is 2500 kg/m3, so magma volume required is

Mass Balance from S and SO_2

Typical SO_2 fluxes from Etna are 3000 tonnes of SO_2 per day

How much magma is needed to produce this gas flux?

SO_2 flux of 3000 t/d = S flux of 1500 t/d (SO$_2$ MW=64g, S AW=32g)

S content of Etnean magma is 0.32 wt%

1500 tonnes = 1.5 million kg of S, divided by 0.32 wt% gives the magma mass:

4.7×10^9 kg of magma required per day

Typical magma density is 2500 kg/m3, so magma volume required is

173,000 m3 of magma per day.

What is Etna doing most of the time, in terms of activity, while processing this voluminous magma supply?

Endogenous growth of persistently active volcanoes

Peter Francis*†, Clive Oppenheimer†
& David Stevenson†

NATURE · VOL 366 · 9 DECEMBER 1993

Endogenous Growth

TABLE 1 Thermal and SO_2 flux data for some persistently active volcanoes

Site/year of observation	Area (m^2)	Effective radiation temperature (°C)	Surface heat flux (MW)	Magma influx model (A) ($kg\ s^{-1}$)	Magma influx model (B) ($kg\ s^{-1}$)	SO_2 flux ($kg\ s^{-1}$)	Magma influx from SO_2 ($kg\ s^{-1}$)	Eruption rate ($kg\ s^{-1}$) (period)
Halemaumau								
1880 (refs 5, 6)	65,100	272	460	3,000	560	—	—	300 (1823–1923)
Kupaianaha								
1987–88 (ref. 8)	2,300	272	16	110	20	—	—	—
Kilauea								
1986 (refs 23, 26)	—	—	—	—	—	13.5 ± 4.6	14,000	~10,000 (Observed recent output)
Stromboli								
1992 (P. Allard)	—	—	—	—	—	9.25	9,300	0.3 (?Since antiquity)
Etna								
1975–1987 (ref. 31)	—	—	—	—	—	46.3 ± 9.0	46,000	~1,000 (1759–1974)
Nyiragongo								
1959 (ref. 18)	13,125	650	620	4,000	750	12.6	13,000	—
Erta 'Ale								
1973 (ref. 19)	7,600	573	260	1,700	320	0.58	580	—
1986 (ref. 32)	30,600	176	100	670	130	—	—	—
Masaya								
1979 (ref. 21)	—	—	—	—	—	13.9	25,000	10 (since 16th C)
Erebus								
1985 (ref. 22)	35,100	137	84	540	100	—	—	—
1987 (ref. 32)	—	—	—	—	—	0.59	590	
Láscar								
1987 (ref. 32)	34,200	171	110	730	140	—	—	450
1989 (ref. 33)	—	—	—	—	—	27.5	28,000	(1984–1993)

Thermal flux estimates are made mostly from satellite observations[32]. Effective radiation temperature is defined as $T_e = (E/\sigma)^{0.25}$, where E is the radiant emittance and σ is the Stefan–Boltzmann constant. Heat fluxes combine radiative and convective losses estimated for the given T_e, but exclude sub-surface conductive and hydrothermal losses. Magma influxes calculated from heat losses are given for models (A) and (B) of Fig. 1. SO_2 fluxes were determined by correlation spectrometer (COSPEC), except for Erta 'Ale and Nyiragongo which were determined by chemical methods. Errors in thermal fluxes are discussed in ref. 32. SO_2 fluxes are reported directly from cited references; errors are often not given. Magma influxes based on SO_2 data were determined for 0.05 wt% degassable sulphur in melt, as at Kilauea, except for Masaya, for which petrological data were available. Eruption rate for Láscar is dominated by the single 1993 eruption volume.

Endogenous growth of persistently active volcanoes

Peter Francis*†, Clive Oppenheimer† & David Stevenson†

NATURE · VOL 366 · 9 DECEMBER 1993

Endogenous Growth

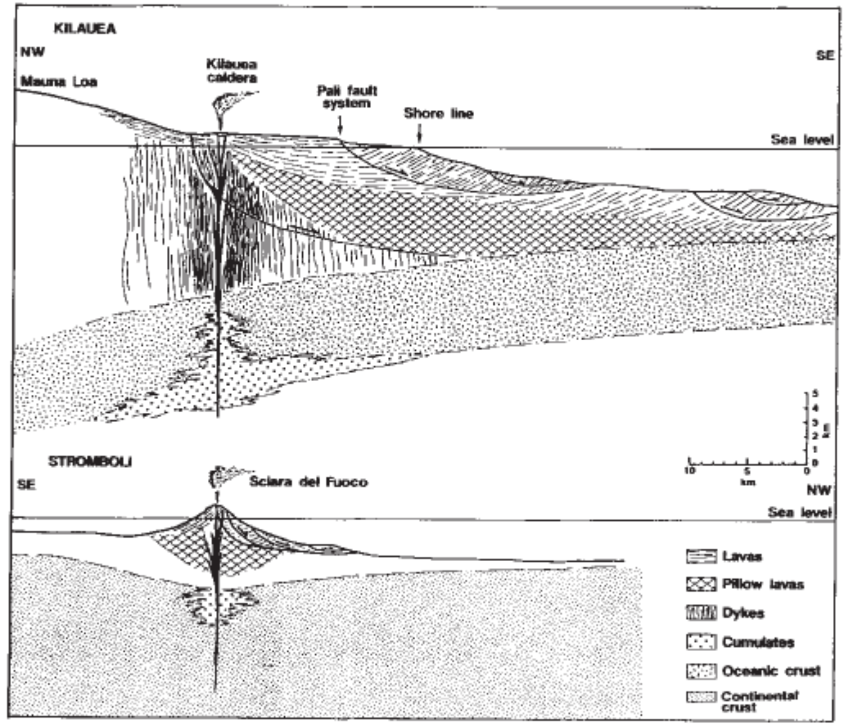

FIG. 2 Cross-sections of Kilauea (top) and Stromboli (bottom) to same scale, showing postulated overall similarities in two-dimensional internal structure, and mode of growth by flank displacement and cumulate formation. Kilauea section from ref. 13, based on seismic data; Stromboli section schematic, based on maps and sections in refs 27 and 28, and sources cited therein. The rotational faults illustrated are based on "shovel-shaped faults" first proposed by Rittman[27]; sub-volcanic cumulates are inferred from geochemical evidence and sections in ref. 28. Lithospheric flexure illustrated is conjectural. Stromboli's geodynamic setting is poorly understood, but the volcano is thought to be constructed on continental crust 15–20 km thick.

Endogenous magma degassing and storage at Mount Etna

Patrick Allard

GEOPHYSICAL RESEARCH LETTERS, VOL. 24, NO. 17, PAGES 2219-2222, SEPTEMBER 1, 1997

Table. Sulfur Output and Magma Degassing Budget of Etna, 1975-1995.

Year	SO_2 output (tons)			Degassed magma (10^6 m^3)			
	Range[§] (10^3/d)	Average[#] (10^6/y)	Eruptive[*] (10^6/y)	Erupt. V_E	Unerupt.[¶] V_U	Total V_D	V_U/V_D
1975	2.7-4.8	1.5	0.07	13	252	265	0.95
1976	1.3-12.4	1.5	0.09	16	249	265	0.94
1977	1.0-5.5	1.5	0.08	15	250	265	0.94
1978	3.2-4.3	1.5	0.28	49	216	265	0.81
1979	0.8-1.5	1.5	0.04	8	257	265	0.97
1980	2.5-6.3	1.5	0.01	3	262	265	0.99
1981	4.0-8.0	1.5	0.19	34	231	265	0.87
1982	9.0-11.5	1.5	0	0	265	265	1.00
1983	2.2-3.3	1.5	0.57	100	165	265	0.62
1984	4.3-5.5	1.5	0.06	10	255	265	0.96
1985	2.4-4.2	1.5	0.18	31	234	265	0.88
1986	-	1.5	0.25	44	221	265	0.83
1987	0.9-10.9	1.6	0.11	20	262	282	0.93
1988	2.7-11.7	2.0	0	0	353	353	1.00
1989	1.0-26.6	2.5	0.43	38	182	220	0.83
1990	2.2-26.3	2.8	0.25	22	225	247	0.91
1991	0.8-16.1	1.8	0.06	10	307	317	0.97
1992	1.0-16.8	2.1	1.19	210	160	370	0.43
1993	2.9-16.2	2.0	0.08	15	338	353	0.96
1994	1.4-12.6	1.8	0	0	317	317	1.00
1995	1.0-11.9	1.6	0	0	282	282	1.00
Σ		36.2	3.95	637	5284	5921	0.89
mean/yr		1.7	0.19	30	251	282	

Excessive degassing of Izu-Oshima volcano: magma convection in a conduit

Kohei Kazahaya, Hiroshi Shinohara, Genji Saito

Bull Volcanol (1994) 56:207–216

Magma Convection In a Conduit

Izu-Oshima is an active basaltic volcano in Japan. The activity of the volcano is characterized by a repetitive cycle consisting of (1) a dormant period, (2) a lava fountaining period, and (3) an active degassing period

Table 2. List of parameters for eruptive and degassing activity of Izu-Oshima volcano during 1950–1974 and 1986–1990

Magmatic activity parameters	1950–1974	1986–1990
Eruptive product (kg)	6.6×10^{10} * (Jul. 1950–Apr. 1951)	3.5×10^{10} ** (Nov. 1986)
Duration of degassing (days)	1400*** (Aug. 1970–Jun. 1974)	800# (Jan. 1988–Mar. 1990)
H_2O flux (kg/s)	—	160
H_2O content of magma (wt%)	—	1.0
SO_2 flux (kg/s)	4.0##	5.0$
S content of magma (ppm)	270$$	270
Mass rate of the magma degassing (kg/s)	$> 7 \times 10^3$	$> 1 \times 10^4$
Total mass of degassed magma (kg)	$> 9 \times 10^{11}$	$> 7 \times 10^{11}$
Unerupted/erupted ratio	>14	>20

* Morimoto (1958), ** Nagaoka (1988), *** Ando (1992), # Kazahaya et al. (1993), ## Okita and Shimozuru (1974), $ Kyushu University (1990), and $$ value assumed to be equal to that of 1986–1990

Excessive degassing of Izu-Oshima volcano: magma convection in a conduit

Kohei Kazahaya, Hiroshi Shinohara, Genji Saito

Bull Volcanol (1994) 56:207–216

Magma Convection in a Conduit

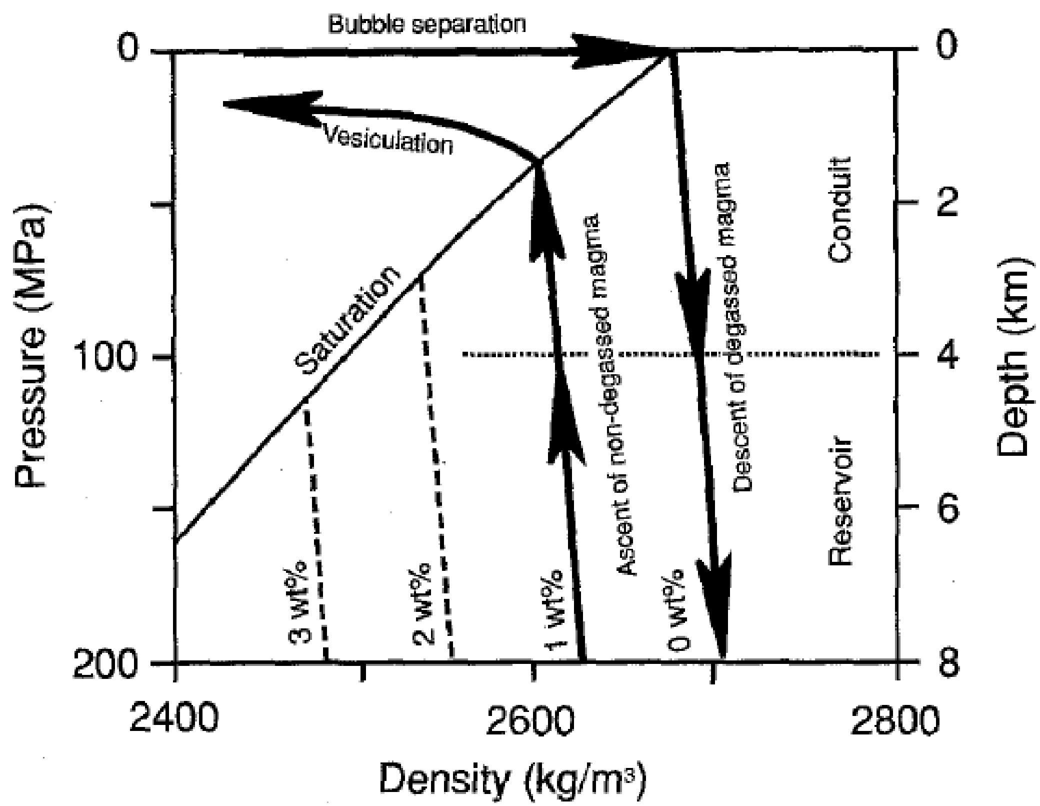

Fig. 1. Density changes of ascending non-degassed magma and descending degassed magma as functions of depth. *Arrows* schematically show a path for the convective transport of magma caused by this density change. *Numerals* show water content in wt%

Bull Volcanol (1994) 56:207–216

Excessive degassing of Izu-Oshima volcano: magma convection in a conduit

Kohei Kazahaya, Hiroshi Shinohara, Genji Saito

Magma Convection in a Conduit

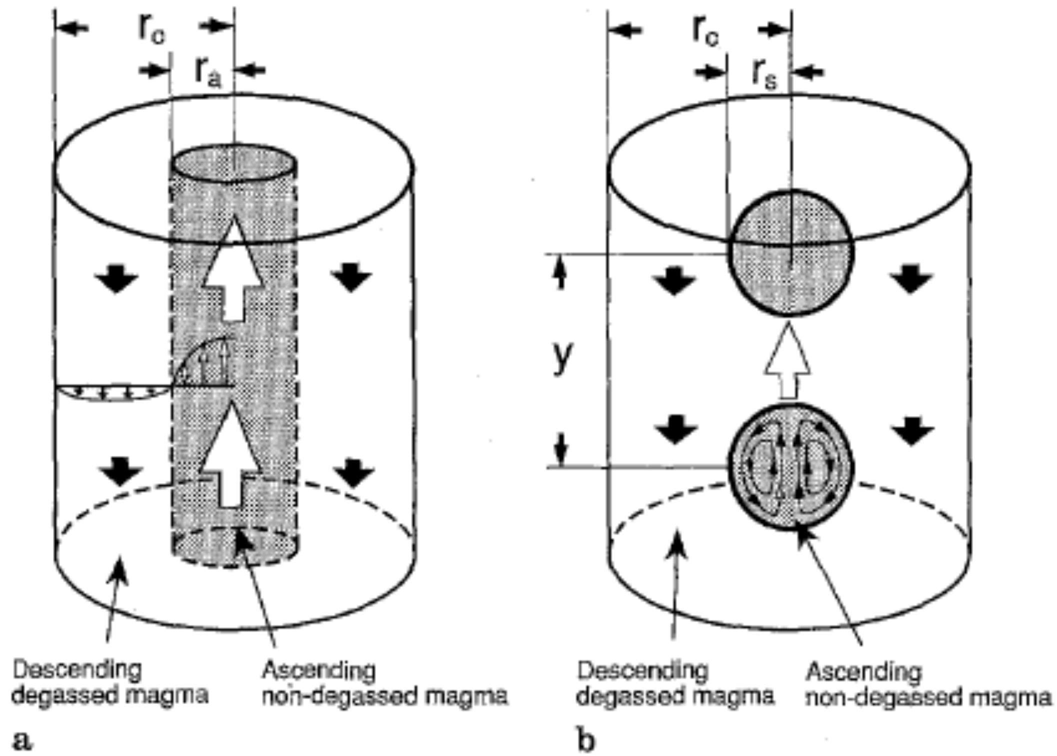

Fig. 2a, b. Schematic diagrams showing magma transport models: **a** Poiseuille flow in a concentric double-walled pipe and **b** ascent of non-degassed magma spheres through the degassed magma column

Is there any evidence for the accumulated degassed magma?

Is there any evidence for the accumulated degassed magma?

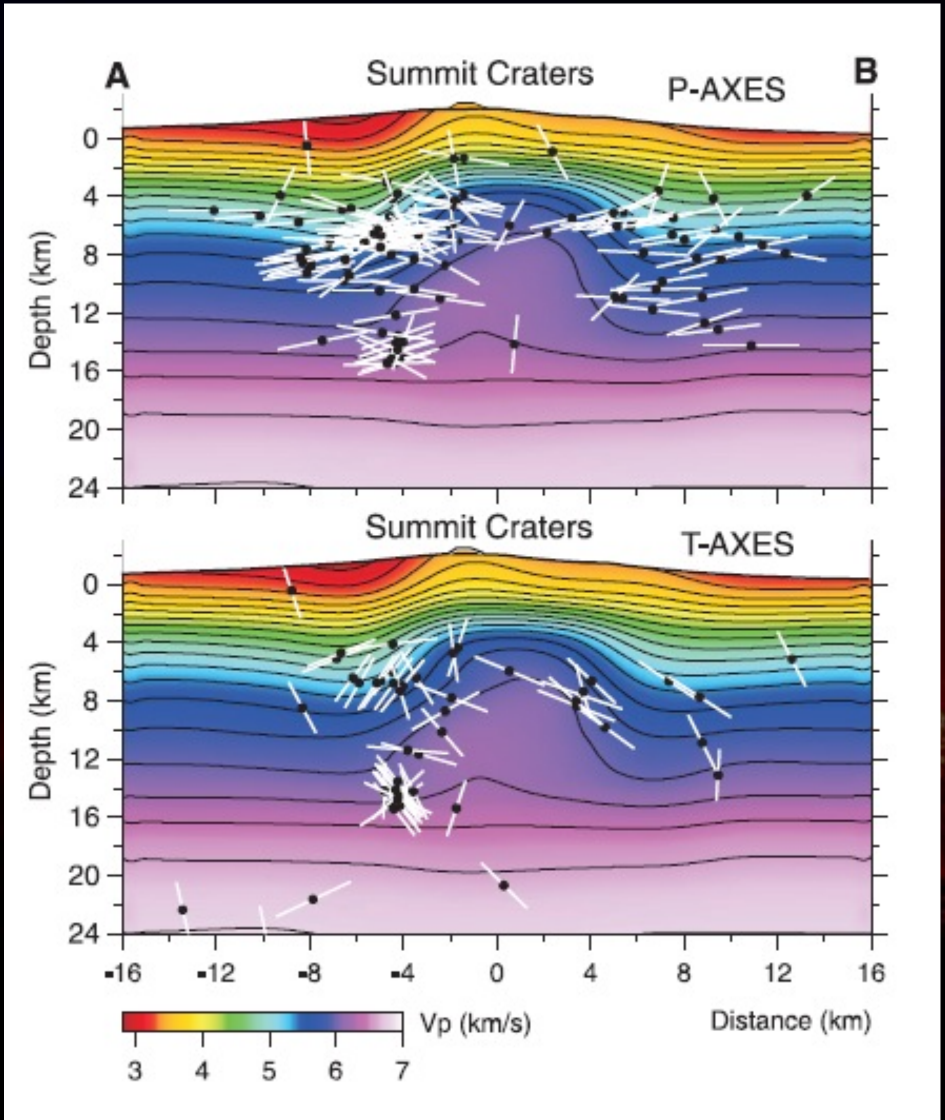

Magma Ascent and the Pressurization of Mount Etna's Volcanic System

Domenico Patanè,[1*] Pasquale De Gori,[2] Claudio Chiarabba,[2] Alessandro Bonaccorso[1]

SCIENCE VOL 299 28 MARCH 2003

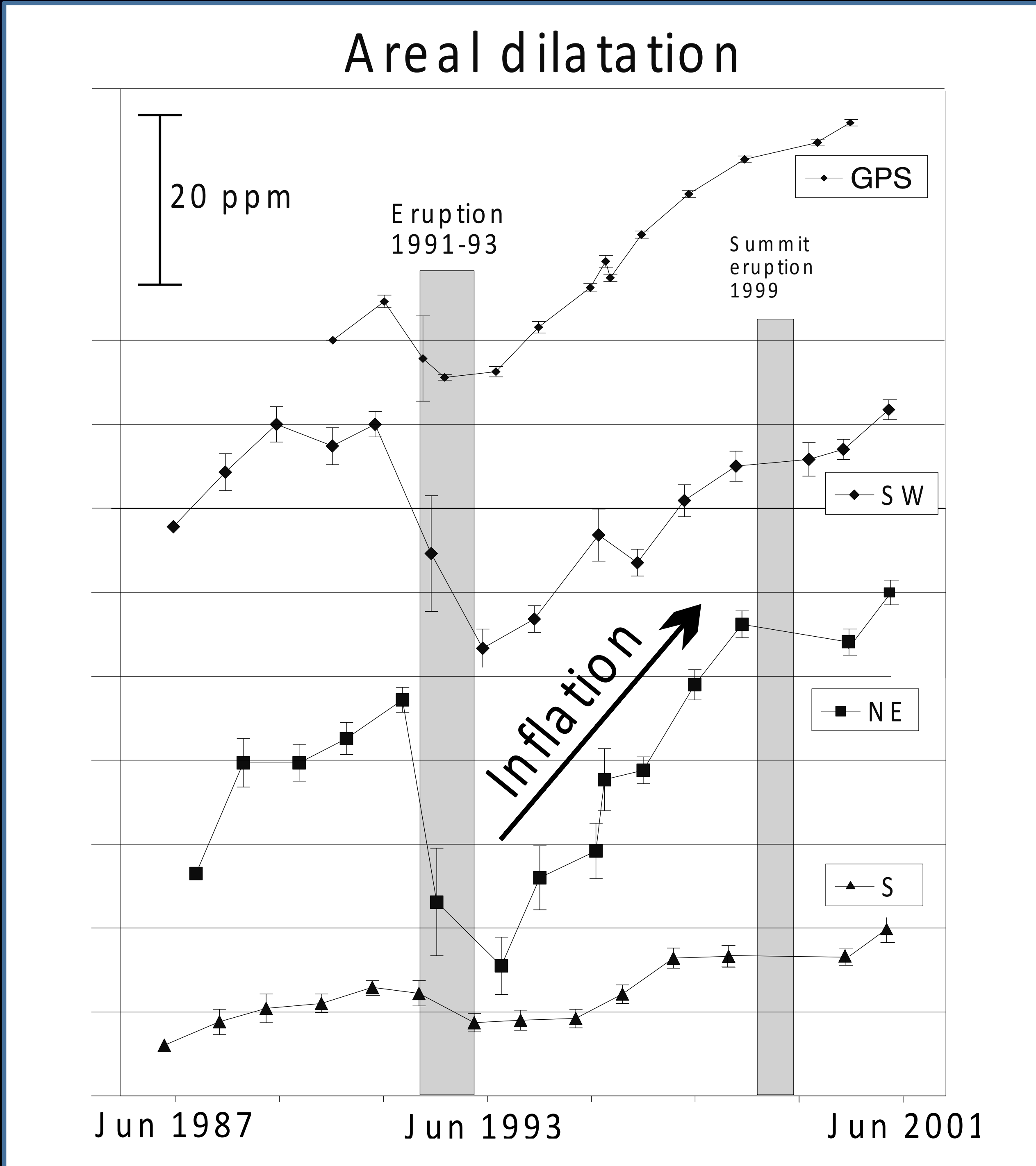
Areal dilatation
20 ppm
Eruption 1991-93
Summit eruption 1999
GPS
S W
N E
S
Inflation
Jun 1987
Jun 1993
Jun 2001

Parameter	Total volumes 1993-2001 (million m^3)	Average volume rates (million m^3/ year)
Deformation source ΔV	216	27
Unerupted degassed magma volume	1030	129
Erupted lava and tephra volume	-125	-16

The Mogi model allows observations of ground deformation to be directly related to changes in the volume of a spherical source within a volcanic edifice:

$$\Delta d = \frac{3\Delta V_{ch}}{4\pi} \frac{d}{(f^2 + d^2)^{3/2}} \quad [1a]$$

$$\Delta h = \frac{3\Delta V_{ch}}{4\pi} \frac{f}{(f^2 + d^2)^{3/2}} \quad [1b]$$

Where *d* is the radial distance at the surface from the centre of a deforming source at depth *f* and *DVch* is the modelled change in volume of the source. Note that *DVch* is implicitly the result of a magma intrusion, but that the volume of injected magma (*DVmagma*) is not necessarily equivalent to *DVch*.

In order to compare *DVmagma* with *DVch* we use the work of Johnson [1992], who examined the dynamics of magma storage on Kilauea volcano, assuming a Mogi source. In such conditions, the change of volcanic edifice volume *(DVedifice*) can be estimated by integrating the equation (1b) on the free surface. This relate the *(DVedifice*) and the change of the source volume (*DVch*) as follows (Johnsonn, 1992):

$$\Delta V_{edifice} = 2(1-\nu)\Delta V_{ch}$$

Johnson [1992] demonstrated that if the volume of injected magma injected into a magma reservoir (*DVmagma*) is much smaller than the reservoir itself, then :

$$\frac{\Delta V_{edifice}}{\Delta V_{magma}} = \frac{2(1-\nu)}{\left\{1+\dfrac{4\mu}{3K_m}\right\}}$$

Where n is the Poisson's ratio, m is the shear modulus of the host rock and K*m* is the (gas free) bulk modulus of the injected magma.

$$\frac{\Delta V_{magma}}{\Delta V_{ch}} = 1 + \frac{4\mu}{3K_m}$$

The compressibility of magma is related to its bulk modulus and may be theoretically estimated, starting from chemical compositions by applying the Lange and Carmichael (1990) model based on the thermodynamic equilibrium of silicate melts, which is in the form of

$$K_T = \frac{V_T}{(dV/dP)}$$

Where *VT* is the volume of a mole of magma at the melt temperature T and *dV/dP* is the volume gradient with respect to the litostatic pressure. For magma having a chemical composition similar to that erupted on Etna in 2001 and 2002-03, Km may be estimated to be ~16 GPa, u is 10-20 GPa

$$\frac{\Delta V_{magma}}{\Delta V_{ch}} = 1 + \frac{4\mu}{3K_m}$$

So for expected values of u and K we expect a ratio of ~4

This means we should see a volume change in terms of deformation 4 times smaller than the volume of injected magma, due to compression and crustal rigidity.

Parameter	Total volumes 1993-2001 (million m^3)	Average volume rates (million m^3/year)
Deformation source ΔV	216	27
Unerupted degassed magma volume	1030	129
Erupted lava and tephra volume	-125	-16

Main Point

• Persistently active volcanoes can produce far more gas than is expected based on their erupted magma volumes, based on mass balance calculations and original/final volatile contents

• This observation implies than endogenous growth takes place, a process that appears to be evidenced by the large plutonic zone under Etna, and is supported by edifice inflation

• Magma convection appears to be the best candidate for explaining this process, whereby ascending magma can quiescently release its volatiles producing a dense degassed magma that sinks back down the conduit in a continuous flow

That’s fluxes.

Now a look at gas compositions with OP-FTIR

FTIR: Introduction

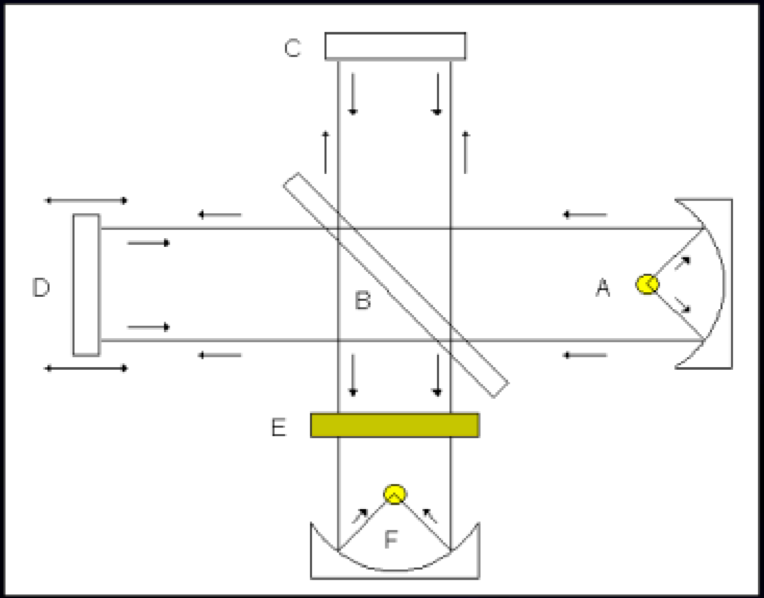

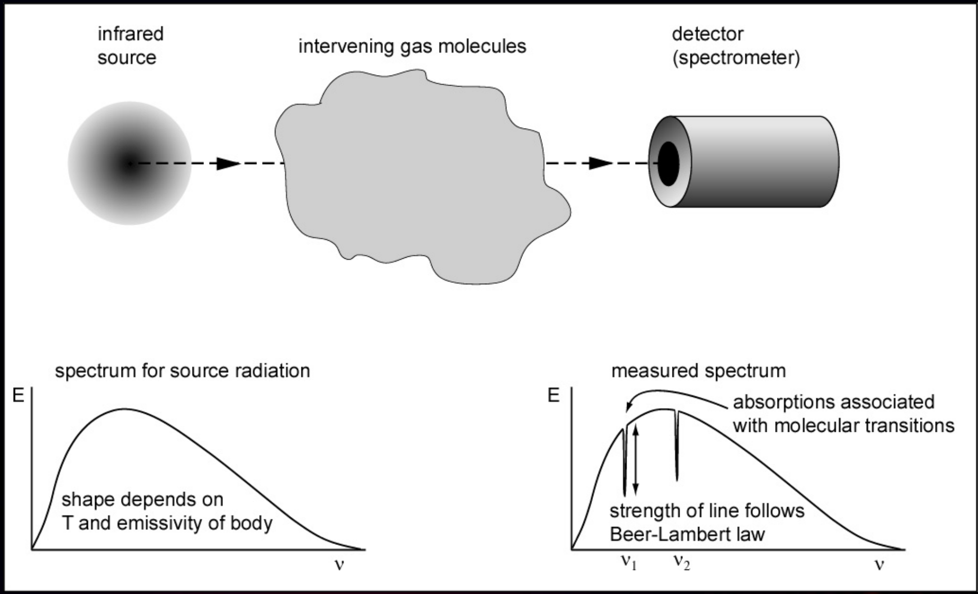

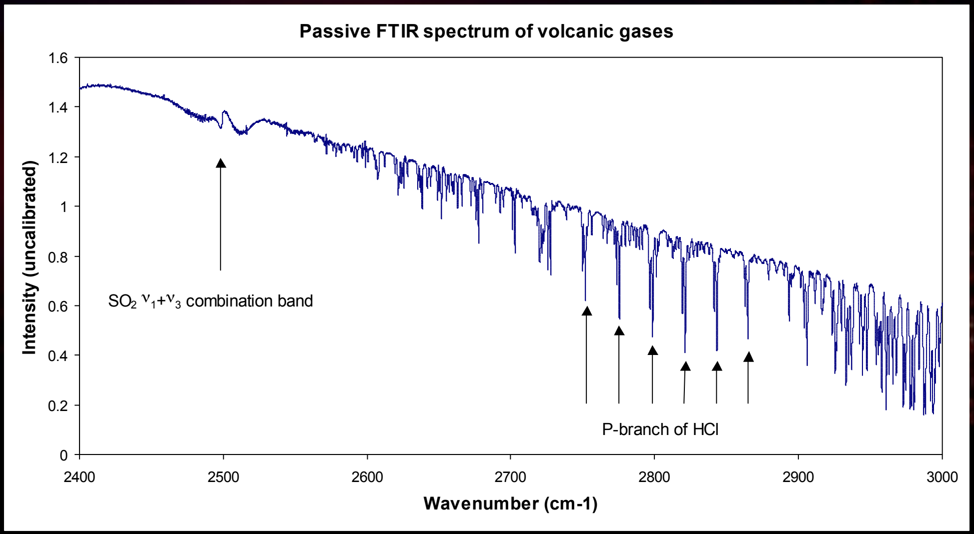

FTIR: Masaya

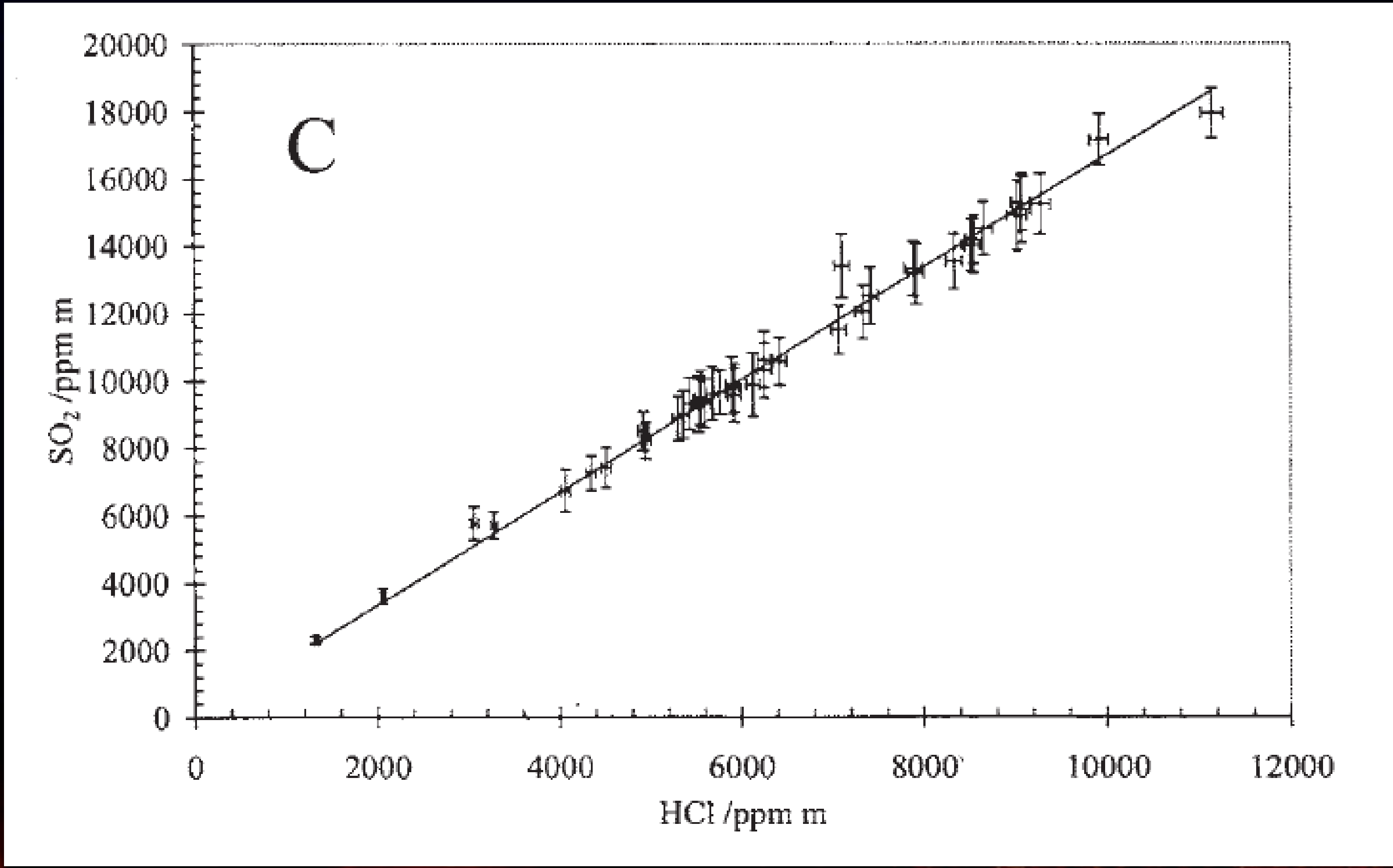

Burton et al., Geology, 2000

FTIR: Masaya

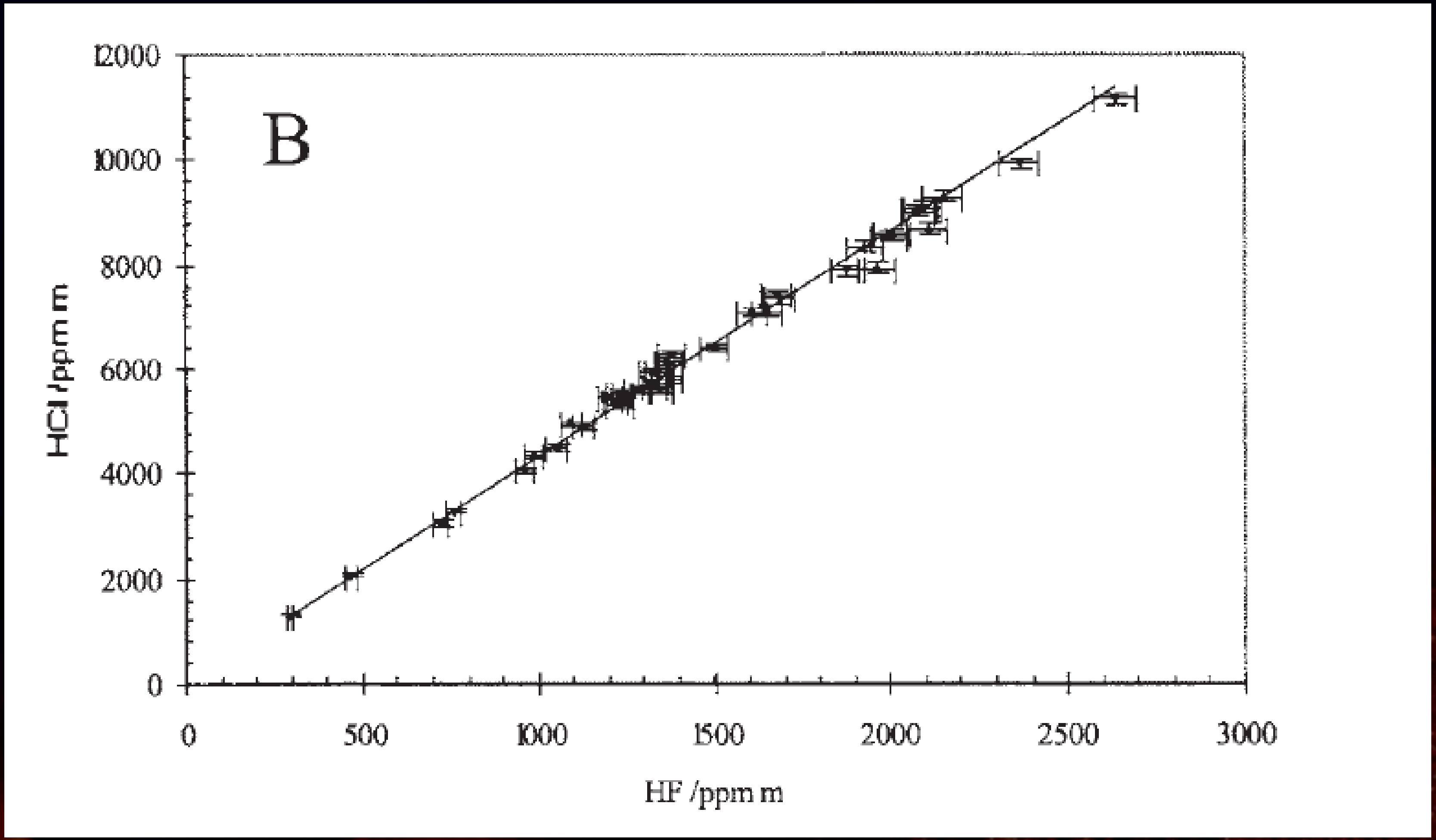
B
12000
10000
8000
6000
4000
2000
0
HCl /ppm m
0
500
1000
1500
2000
2500
3000
HF /ppm m

FTIR: Masaya

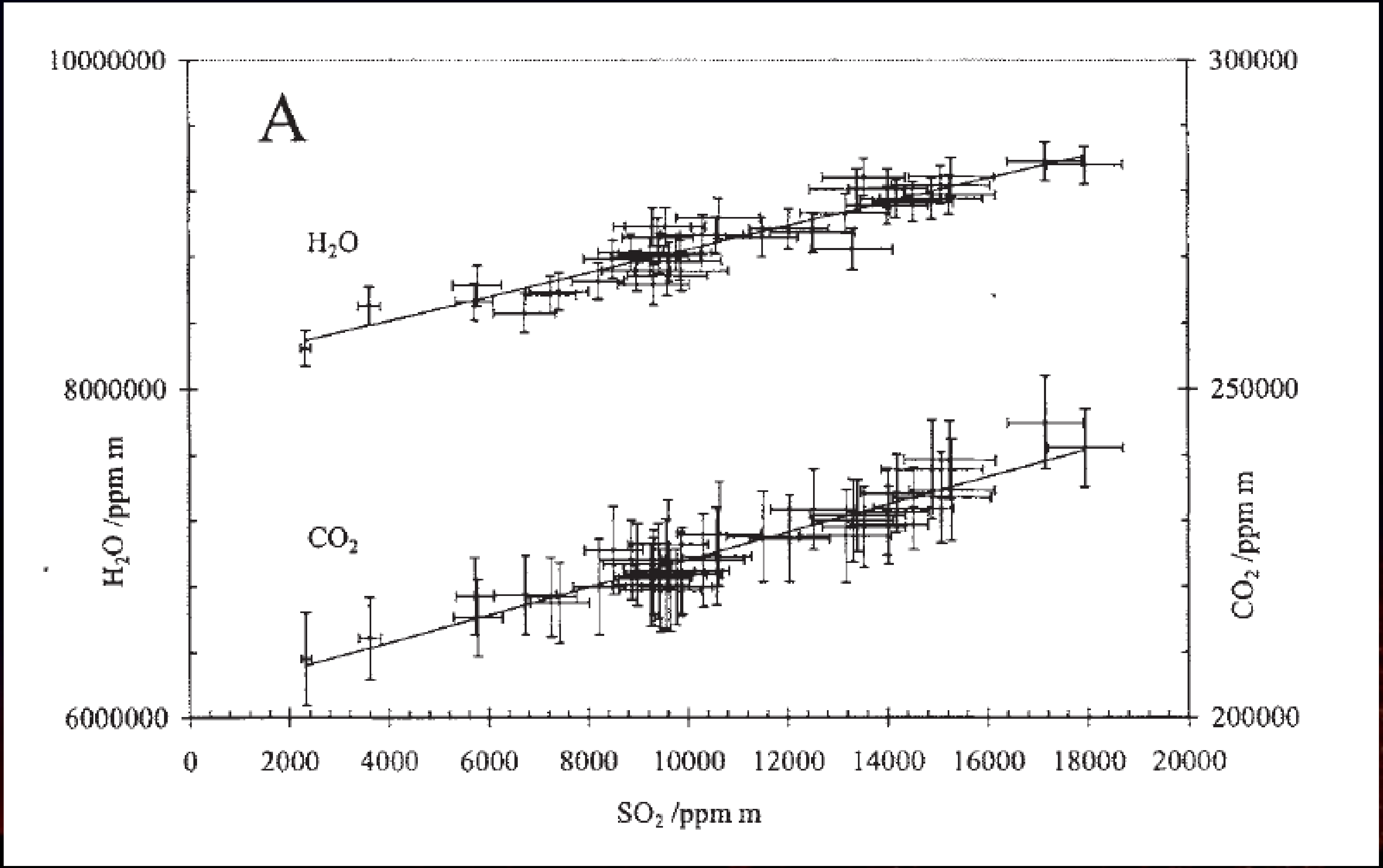

A
H_2O
CO_2
10000000
8000000
6000000
300000
250000
200000
0
2000
4000
6000
8000
10000
12000
14000
16000
18000
20000
H_2O /ppm m
CO_2 /ppm m
SO_2 /ppm m

FTIR: Masaya

TABLE 2. GAS COMPOSITION OF MASAYA PLUME AND OTHER BASALTIC CENTRAL AMERICAN ARC VOLCANOES

Gas	Masaya 1998	Masaya 1999	Poás 1981	Momotombo 1980
H_2O	94.20	94.26	96.16	97.11
H_2	–	–	0.54	0.70
CO_2	3.37	3.25	0.99	1.44
CO	–	–	0.01	0.01
SO_2	1.37	1.434	1.45	0.50
H_2S	–	–	0.01	0.23
HCl	0.87	0.85	0.75	2.89
HF	0.19	0.19	0.09	0.16

Note: Data for Poás (Costa Rica) and Momotombo (Nicaragua) are restored analyses for the highest temperature samples provided in Symonds et al. (1994). All analyses in mol%.

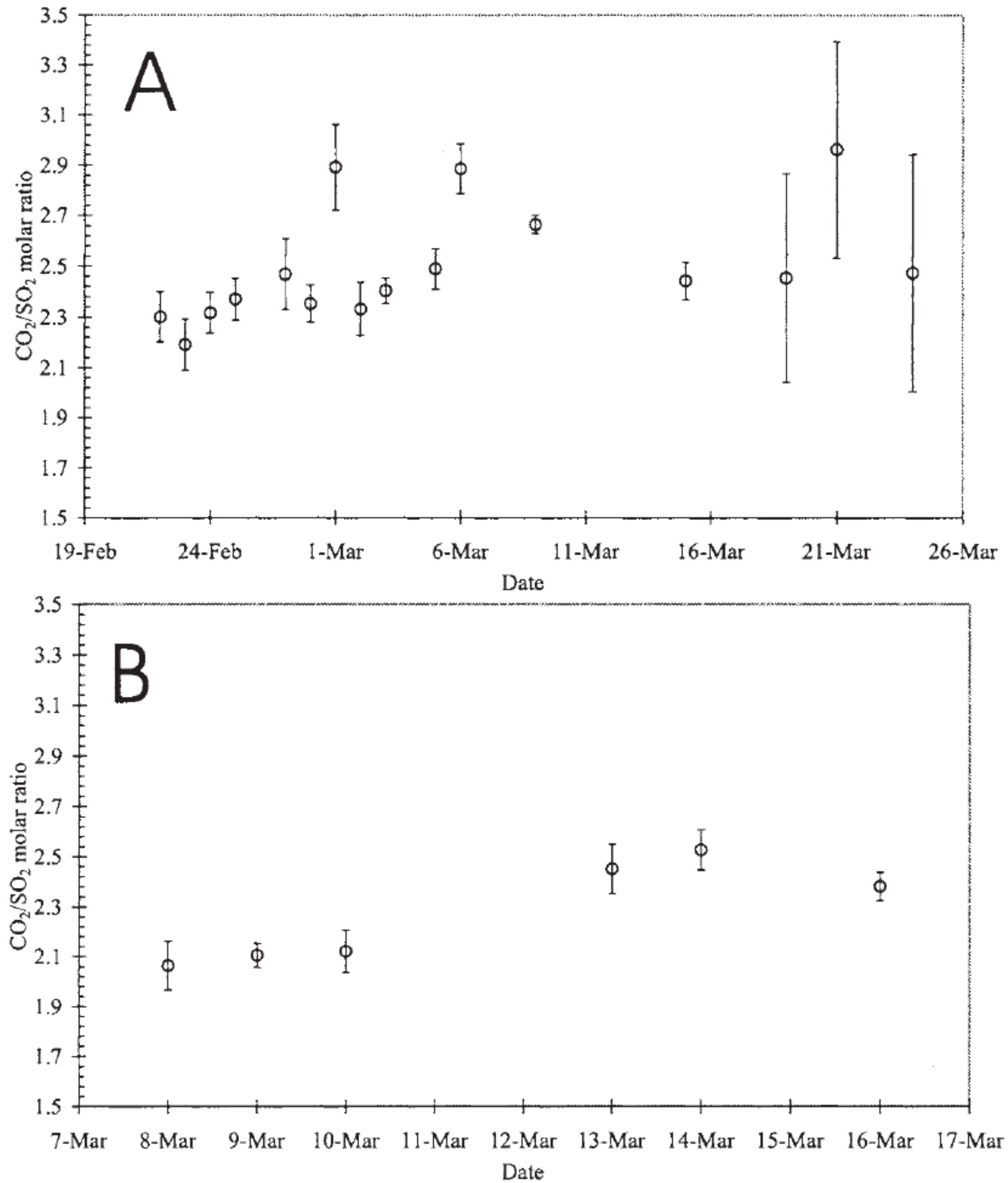

Figure 3. CO_2:SO_2 ratio in (A) February–March 1998; (B) March 1999, illustrating limited variation over 1 yr period.

FTIR: Stromboli Explosions

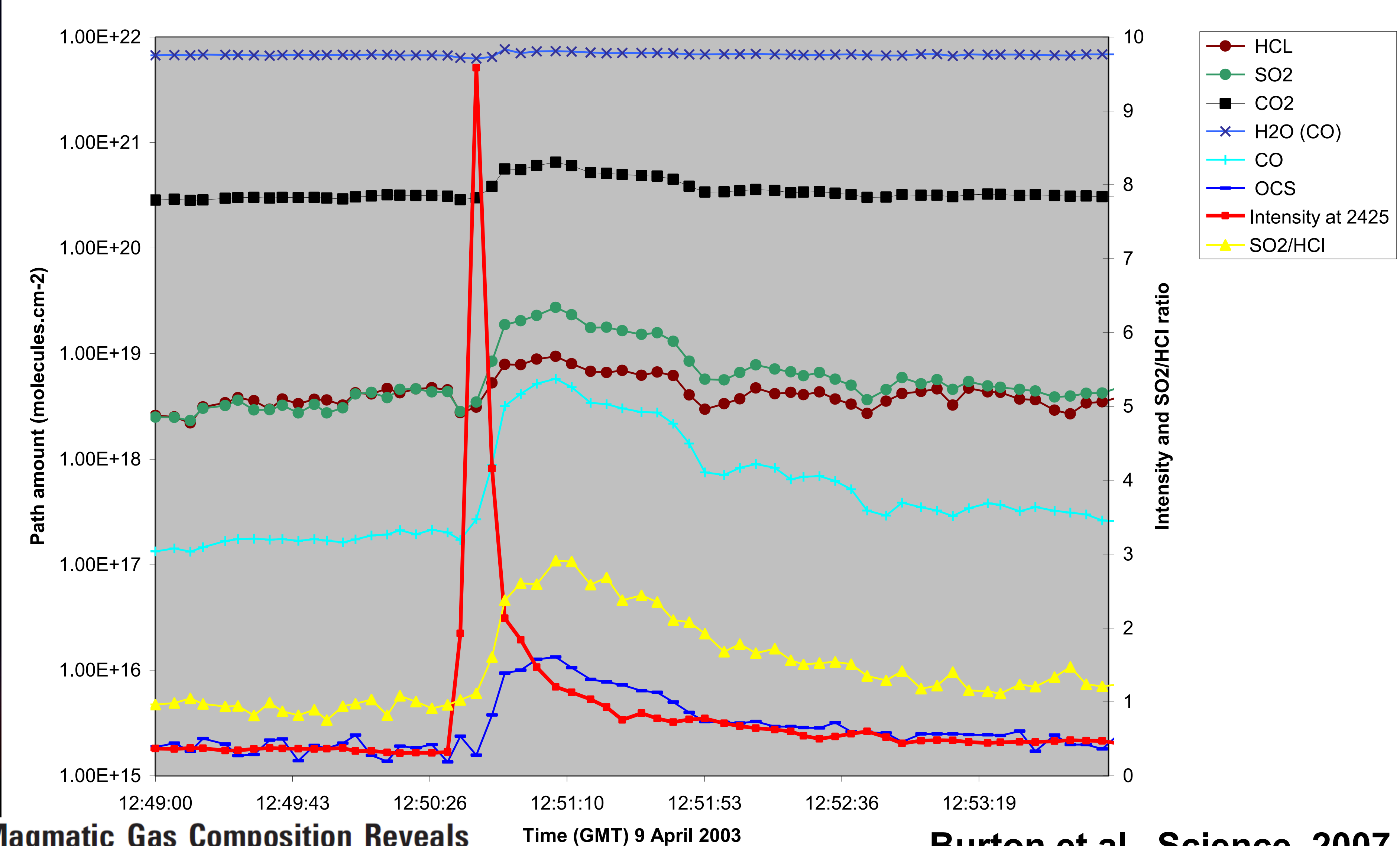

Burton et al., Science, 2007

Magmatic Gas Composition Reveals the Source Depth of Slug-Driven Strombolian Explosive Activity

Mike Burton,[1*] Patrick Allard,[1,2] Filippo Muré,[1] Alessandro La Spina[1,3]

FTIR: Stromboli Explosions

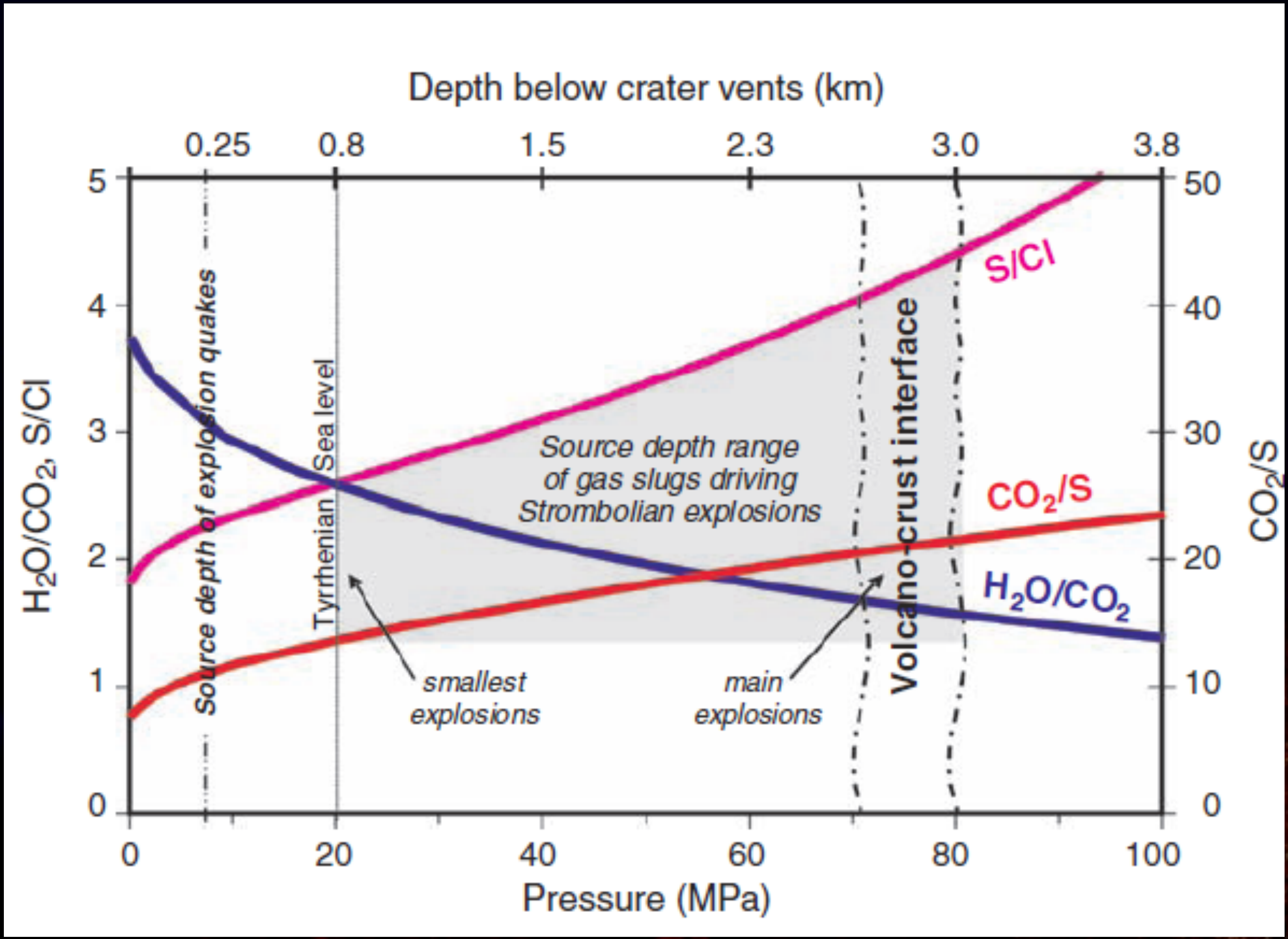

Magmatic Gas Composition Reveals the Source Depth of Slug-Driven Strombolian Explosive Activity

Burton et al., Science, 2007

FTIR: Mt. Etna plumbing system

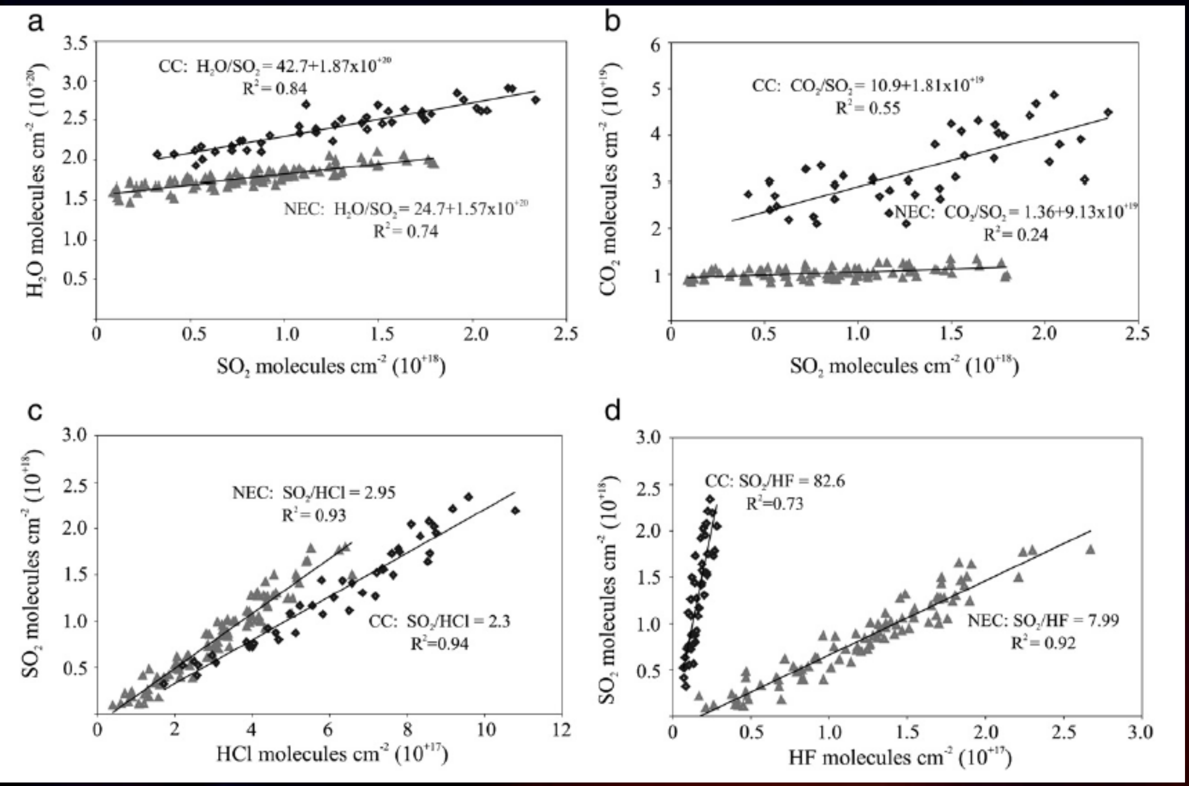

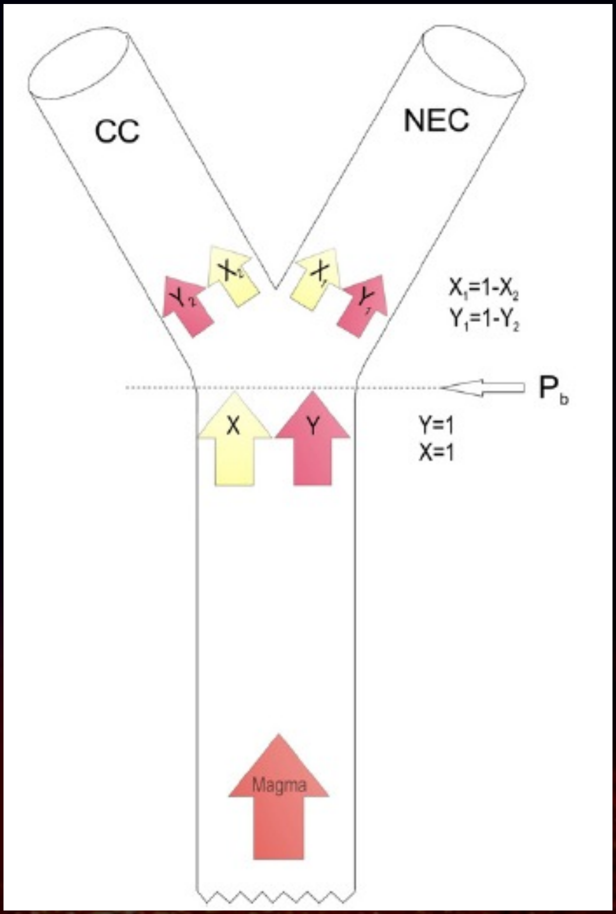

High and low CO2/SO2 gas ratios emitted from two main craters of Etna, consistent with conduit branching 1-3 km below surface

Unravelling the processes controlling gas emissions from the central and northeast craters of Mt. Etna

Journal of Volcanology and Geothermal Research 198 (2010) 368–376

Alessandro La Spina [a,b,*], Mike Burton [c], Giuseppe Giovanni Salerno [b,d]

Conclusions

- Gas measurements give complimentary information about the volcanic system
- There has been a rapid evolution in gas monitoring capacity in last 10-15 years
- SO2 camera offers real advantages in quantifying SO2 compared with existing methods: need to rethink strategies.
- Much further work to be done in mass balance investigations.